Some Mineralogical Characteristics of the Egyptian Black Sand Beach Ilmenite Part II: Rutile-Ilmenite and the Various Titanhematite Grains

Mohamed Ismail Moustafa
Northern Border University, Saudi Arabia and
Nuclear Materials Authority, Cairo, Egypt
ismail2251962@yahoo.com

Received: 30 August 2022 | Revised: 15 September 2022 | Accepted: 17 September 2022

Abstract-In addition to the grains of homogeneous ilmenite, ferriilmenite, hematite-ilmenite exsolved intergrowths, and the partially altered ilmenite grains, other textures are detected in the separated ilmenite concentrate. The grains of rutile-ilmenite exsolved intergrowth represent 0.8% of the detected ilmenite grains. The ilmenite component of this intergrowth is detected to be ferriilmenite associated with geikielite, pyrophanite, and rutile, with Cr_2O_3 content ranging between 0 and 0.5%. The exsolved rutile is ferriforrous rutile composed of rutile, hematite, geikielite, and pyrophanite, its Cr_2O_3 content ranging between 0 and 0.4%. The detected individual titanhematite grains represent 4.4% and include 3 textures arranged, in a decreasing order of abundance, as: ilmenite-hematite, rutile-hematite, and rutile-ilmenite-hematite exsolution intergrowths. MgO and MnO have minimum values and they do not follow Fe_2O_3. In some homogeneous titanhematite or exsolved rutile-hematite, Fe_2O_3 content may be replaced with SiO_2. In all titanhematite intergrown textures, the Cr_2O_3 content ranges between 0 and 0.1%. Only in the case of the titanhematite host with exsolved rutile, the contained MgO ranges between 1.2 and 5.3%. Some ferromagnetic titanhematite grains separated with the fraction of magnetite are detected. In these grains, the Cr_2O_3, MgO, and MnO contents range between 0-0.2, 0-3, and 0-1.4% respectively. Several varieties of chromite and chromspinel mineral grains are found and represent 1.1% of the detected bulk ilmenite grains. In these grains, the Cr_2O_3, MgO, V_2O_3, and Al_2O_3 contents range between 16.69-56.72%, 0.54-17.33%, 0.14-0.58%, and 1.33-38.79% respectively. Although they are rarely met in the ilmenite concentrate, the relatively finer grain sizes could lead to the separation of some with ilmenite fraction rather than with the ferromagnetic one. It is concluded that the problem of high Cr_2O_3 and Fe_2O_3 contents of the Egyptian beach ilmenite concentrate is not only a mineralogical problem, but also an ore-dressing one.

Keywords-black sands; beach ilmenite; ferriforous rutile; titanhematite; martitization; exsolved intergrowth

I. INTRODUCTION

The placer deposits are very important sources of many economic minerals. The Egyptian black sands extend along the northern coastal stretch between Abu Qir to the west and Rafah to the east. These deposits contain 6 economic minerals: ilmenite, magnetite, garnet, zircon, rutile, and monazite. They are present either as beach sediments or as coastal sand dunes. Ilmenite alone reaches up more than 50% of the total. However, the original amount of materials transported by the river may be related to several variables such as the flow type and the sediment load [1]. Most ilmenite grains are found in fine and very fine sand-sized grains. In fact, the original grain size may affect the rate of mineral alteration [2]. The grain size becomes relatively coarser on moving from Rosetta to the west to Rafah to the east due to drifting by alongshore currents. Ilmenite also occurs in massive rock formations in the form of titaniferous ore, associated with hematite and magnetite [3]. Among the titanium minerals, only ilmenite, leucoxene, and rutile have significant importance [4-7]. The ilmenite ore is the main source for the production of metallic titanium and titanium containing compounds. The mineralogy of the Egyptian beach ilmenite has been studied in [8-15] among others. Many authors reported the relatively lower TiO_2 content and relatively higher Fe_2O_3 and Cr_2O_3 contents and others reported the diversity of the mineralogical textures inside ilmenite grains.

In the Egyptian black sand, the ilmenite content varies from less than 1% in the raw beach sand up to more than 50% in the naturally highly concentrated surfacial black sands. Most of the obtained Egyptian beach ilmenite concentrates are characterized by a relatively lower TiO_2 content (44-46% of ilmenite's beach sand and 46-49% of ilmenite's sand dunes) and relatively greater Cr_2O_3 content (0.1-0.4%). Also, they have a relatively lower Fe^{2+}/Fe^{3+} ratio and relatively higher MgO and MnO contents. Authors in [16] explained that the general break-even grade for ilmenite is considered to be 47 to 48% TiO_2, a rise in the ratio from 51% to 54% TiO_2 will, however, double profits.

The trace element concentrations of ilmenite grains show enrichment in Cr and V contents indicating that these elements are probably hosted by ilmenite [8]. The Cr_2O_3 content is negligible in the lattice of the Egyptian beach ilmenite and hematite. However, up to 0.36% Cr_2O_3 was recorded in the whole concentrate analysis that could be due to accessory Cr-

Corresponding author: Mohamed Ismail Moustafa

spinel minerals. The V content in the Egyptian ilmenite (av. 0.3%), which probably affects the pigment brightness, is relatively high [17]. Hydrometallurgical and/or pyrometallurgical processes for converting the Egyptian beach ilmenite concentrate into a marketable product are investigated in [18-19]. The separation procedures of ilmenite and other economic mineral concentrates of the Egyptian beach sand and other deposits are explained in [15, 20]. To detect the reasons of the relatively higher Cr_2O_3 and Fe_2O_3 content in addition to the relatively lower TiO_2 content of most of the obtained Egyptian beach ilmenite concentrates, most of the contained mineral textures within the ilmenite concentrate, associated with the other obtained magnetic fractions, will be investigated. Knowing such reasons, the process of ilmenite separation, the chemical specification of the obtained ilmenite concentrate, and its corresponding marketable value can be improved.

II. MATERIALS AND METHODS

A bulk sample of about 1000tons was collected from the surfacial naturally highly concentrated beach black sand at the Mediterranean coast, 7km east of the Rosetta estuary. The sample represents the raw sand in a 2km stretch with variable width of a few meters to 20m. The sand was manually scraped from the mantle to a depth ranging between 10-30cm. Using the difference in physical characteristics between the various economic minerals, the collected surfacial naturally highly concentrated beach raw sand was processed using the following equipment: Full- and Half-size Wilfley shaking tables for wet-gravity concentration, Carpco (HP 167) high-tension roll-type electrostatic separator for electrostatic separation, Reading cross–belt magnetic separator, and the Carpco (MIH 13-231-100) industrial high intensity induced roll dry magnetic separator for magnetic separation. Finally, a bulk conductor ilmenite fraction was obtained and was subjected to the refining magnetic stage using the Reading cross-belt magnetic separator, after which an ilmenite concentrate assaying 99.5% ilmenite grains was obtained.

Four polished sections were prepared from 4 small representative samples and were studied under the reflected microscope and Cameca SX-100 microprobe instrument. They were taken from the obtained final ilmenite concentrate (including 2 obtained magnetic fractions of the reading separator), a representative sample of the obtained ferromagnetic fraction, a representative sample of all the other obtained magnetic fractions of the separator, and finally a representative sample of the obtained nonmagnetic fraction of the separator.

The investigation of the different ilmenite grains was carried out by a Cameca SX-100 electron microprobe analyzer (EMPA), from the Institute of Mineralogy and Crystal Chemistry, Stuttgart University, Germany. The microprobe instrument is equipped with 3 Wavelength Dispersive Spectrometers (WDSs) and an Energy Dispersive Spectrometer (EDS). The whole surface of the polished sections was examined by Back Scattered Electron (BSE) images, so that ilmenite grains with 10μm size or even smaller could be detected. The analytical conditions were 15kV accelerating voltage, 15nA electron current, 180s counting time for each analyzed spot in the investigated grains, and 1 to 4μm diameter of the focused electron beam. The following standards were used: diopside for Mg and Ca, albite for Na, corundum for Al, orthoclase for Si and K, rutile for Ti, rhodonite for Mn, Fe_2O_3 for Fe, Cr_2O_3 for Cr, V for V, and sphalerite for Zn. Kα lines were used for analysis. Also, a stereoscopic binocular microscope, a reflected-light polarizing microscope, Jones riffle splitters of various sizes, and containers of varies sizes are used.

III. CALCULATION

The calculation of Fe^{3+} content, the molecular formula of the contained ilmenite mineral components of the studied individual ilmenite grains, the methods of calculation of the different mineral components of the analyzed spots composed mainly of ferriilmenite and/or titanhematite with or without individual TiO_2 (rutile), and the calculation of different mineral components of the analyzed ferriforous rutile are as those of [21].

IV. RESULTS

Homogeneous ilmenite, homogeneous ferriilmenite, hematite-ilmenite exsolved intergrown grains, and the partially altered ilmenite varieties are discussed in [21], while the remaining ilmenite textures are investigated in this paper. Various mineral textures are detected and analyzed. 41 analyzed spots within 7 grains of rutilo-ilmenite exsolved intergrowthed grains are investigated. Several ilmenite grains were detected to enclose rutile exsolution lamellae that are frequently undulating and arranged in one direction and to somewhat similar to what is called “Blitz structure” described in [22]. However, the texture is clearer under crossed nicols and with colored images. The ilmenite chemical molecular formula and the corresponding mineral component fractions are calculated. The detected individual titanhematite grains represent 4.4%. 53 analyzed spots within 8 titanhematite grains were investigated. Normal hematite (pure Fe_2O_3), showing well-defined optical properties under the reflected light is very rare. Titanhemetite is sliglitly greyish white, showing a relatively lower reflectivity and is strongly anisotropic from bright slightly greyish white with pale yellowish tint to dull grey with faint bluish tint, rarely showing red internal reflections. However, titanhematite (Ti-rich hematite) is slightly darker and more greyish white than the primary and secondary hematite formed by martitization of magnetite or by the alteration of ilmenite. The ilmenite-hematite exsolution intergrowth is much less common than the hematite-ilmenite exsolution intergrowth. However, it is considered the most common exsolution intergrowth in the host titanhematite grains. In the present study, the host titanhematite mineral grain encloses exsolved lamellae of ferriilmenite oriented with their long axes parallel to the (0001) plane (Figure 1(1)).

On the other hand, some titanhematite grains contain 2 distinct size classes of ferriilmenite exsolution lamellae, an ordinary and a coarse type of intergrowth. In both cases, relatively finer ferriilmenite exsolution bodies are observed between the coarser bodies. Also, the very coarse ferriilmenite exsolution bodies may in turn contain very fine lamellae of titanhematite (Figure 1(2)). The same phenomenon was

observed in [23]. In rare cases, twinned ferriilmenite-titanhematite individual components are observed where the exsolved ferriilmenite lamellae are arranged parallel to the (0001) plane of the host titanhematite in each component which has different oriented direction (Figure 1(3)). Also, some rare composite grains, consisting of differently oriented titanhematite grains are observed with exsolutions of ferriilmenite parallel to their basal planes (Figure 1(4)). Sometimes narrow rims or small parts of homogenous ilmenite occur on the borders of these titanhematite grains. Some of these titanhematite grains can also contain fine exsolution lamellae of rutile parallel to one or more of its ($22\bar{4}3$) directions.

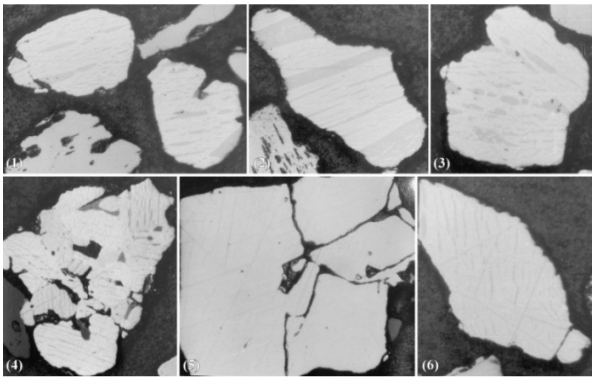

Fig. 1. Various ferriilmenite-titanhematite exsolved intergrowth samples, sometimes including rutile exsolved bodies: (1) Ferriilmenite-titanhematite exsolution intergrowth with the exsolved ferriilmenite lamellae parallel to the (0001) plane of titanhematite. Reflected light, ×100. (2) Two different sizes of exsolved ferriilmenite in the host titanhematite. The relatively coarser exsolved ferriilmenite lamellae contain very fine exsolved lamellae of titanhematite. Reflected light, ×100. (3) Two twinned ferriilmenite-titanhematite exsolution intergrowths. The exsolved ferriilmenites show different oriented directions in relation to each other. Reflected light, ×100. (4) Granular aggregates of differently oriented titanhematite crystals, each of them containing exsolved ferriilmenite lamellae parallel to its basal plane. Some of them also contain fine lamellae of exsolved rutile. Reflected light, ×100. (5) Titanhematite (greyish white) with rutile exsolutions (light grey) parallel to the ($22\bar{4}3$) direction. Reflected light, ×100. (6) Ferriilmenite-titanhematite exsolution intergrowth associated with exsolved rutile needles. The exsolved ferriilmenite (dark grey) is parallel to the (0001) direction, while the exsolved rutile (light grey) is parallel to the ($22\bar{4}3$) direction. Reflected light, ×100.

The second common exsolution intergrowth in the host titanhematite is rutile-titanhematite intergrowth. A considerable number of the detected titanhematite grains are not free of rutile exsolved lamellae. Fine needles of exsolved rutile were observed in up to 6 directions parallel to the ($22\bar{4}3$) planes of the titanhematite (Figure 1(5)). The third common exsolution intergrowth in the host titanhematite is rutile-ilmenite-hematite exsolution intergrowth. In this case, some of titanhematite grains contain exsolved ferriilmenite lamellae which are pod-shaped or spindle-shaped and are oriented in one direction parallel to the (0001) plane of the titanhematite. The exsolved ferriilmenite lamellae are associated with the exsolved fine needles of rutile which are arranged along 1, 2 to 6 directions, parallel to the ($22\bar{4}3$) planes of the titanhematite, and are much more elongated than the exsolved ferriilmenite (Figure 1(6)). In most cases, the exsolved rutile needles cut the grain from side to side and are oblique to the direction of the ferriilmenite lamellae. The corresponding different mineral component fractions of the all the analyzed spots are calculated.

Finally, 49 analyzed spots within 6 grains of ferromagnetic titanhematite associated with magnetite in its ferromagnetic fraction were detected. The hematite chemical formula and the corresponding mineral component fractions were calculated. Some of analyzed spots are corresponding to impurities of silica, calcite, altered silicate minerals, and pseudobrookite. The analyzed oxides of the detected spots include TiO_2, FeO, Fe_2O_3, Cr_2O_3, MnO, MgO, Al_2O_3, V_2O_3, ZnO, SiO_2, and CaO.

V. DISCUSSIONS

A. Rutile-Ilmenite Exsolution Intergrowth (0.8%)

The rutile exsolutions in ilmenite are far less common than in titanhematite. These intergrowths of exsolved rutile are possibly the result of unmixing of a rutile-ilmenite solid solution, which must be very limited as the observed rutile lamellae are very few in number, extremely fine, while the intergrowth is very rare [14, 23-24]. This is in accordance with the results obtained in [25] for synthetic preparations, that not more than 6% TiO_2 can exist in solid solutions in ilmenite at 1050°C. However, 6 grains were detected for this exsolution intergrowth and their chemical compositions were investigated with the microprobe. It is noticed that the content of the exsolved rutile is relatively higher than that recorded in previous studies.

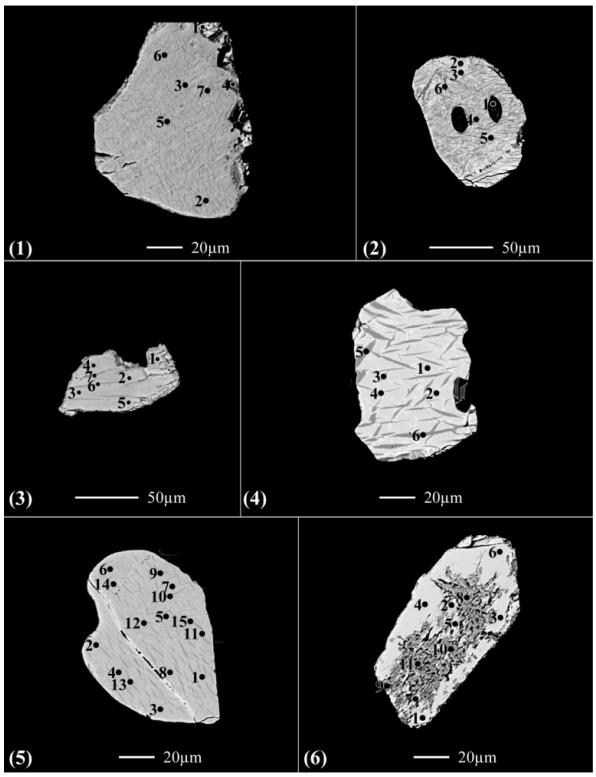

Fig. 2. BSE images of various rutilo-ilmenite exsolved intergrowth grains.

Spots 2, 3 of grain (1) of Figure 2 (Table I), are ferriilmenite with considerable amounts of geikielite and minor pyrophanite and rutile in solid solutions. In these spots, the first method (M1) of calculation is used to calculate the different mineral fractions of the two spots. Then, the mineral components of the two spots are: Spot 2: 64.42% ilmenite, 22.9% hematite, 11.03% geikielite, 1.28% pyrophanite, and 0.16% rutile and spot 3: 66.11% ilmenite, 21.60% hematite, 10.14% geikielite, 1.28% pyrophanite, and 0.15% rutile.

Spot 1 of grain (1) of Figure 2 (Table II) is titanhematite with considerable amounts of rutile and geikielite. It is composed of 69.48% hematite, 11.63% geikielite, 1.7% pyrophanite, and 16.9% rutile. Spot 4 is mostly ilmenite. Spots 5-7 of grain (2) of Figure 2 (Table II) are ferriferous rutile composed mostly of rutile with considerable amounts of hematite (Fe_2O_3), ranging between 21.91% and 33.86%, geikielite, and pyrophanite mineral components. In these spots, the third method (M3) of calculation is used to calculate the different mineral fractions. Their mineral components are: Spot 5: 33.86% hematite, 6.09% geikielite, 0.64% pyrophanite, and 58.59% rutile, spot 6: 27.62% hematite, 4.18% geikielite, 0.53% pyrophanite, and 67.21% rutile, and spot 7: 21.91% hematite, 2.42% geikielite, 0.43% pyrophanite, and 73.22% rutile. It is obvious that the content of TiO_2 (rutile) decreases as the content of geikielite and pyrophanite increases. The same relation is detected between the exsolved rutile and the mixed hematite inside it.

TABLE I. MICROPROBE CHEMICAL ANALYSIS AND MOLECULAR FORMULAE OF THE ANALYZED SPOTS FOR THE RUTILO-ILMENITE EXSOLVED INTERGROWN GRAINS OF FIGURES 2, 3

Grains	Spot	SiO_2	MgO	MnO	CaO	ZnO	FeO	Al_2O_3	V_2O_3	Cr_2O_3	TiO_2	Total	FeO	Fe_2O_3	Total	Fe^{2+}	Fe^{3+}	Other cations	Ti	O	Gek	Pyr	Ilm	H	R	Total
Fig. 2 (1)	2	0.00	3.70	0.60	0.00	0.10	50.60	0.20	0.50	0.40	42.20	98.30	30.50	22.30	100.50	0.63	0.41	0.19	0.78	3	11.03	1.28	64.42	22.90	0.16	99.79
	3	0.00	3.40	0.60	0.00	0.10	50.20	0.20	0.50	0.40	42.20	97.50	31.30	21.00	99.60	0.65	0.39	0.17	0.79	3	10.14	1.28	66.11	21.60	0.15	99.27
	4	0.70	0.20	0.40	0.10	0.00	41.10	0.10	0.60	0.50	52.50	96.30	41.10	0.00	96.30	0.90	0.00	0.07	1.03	3	0.60	0.85	86.80	0.60	5.89	94.74
Fig. 2 (2)	2	0.00	5.10	0.70	0.00	0.00	53.30	0.40	0.40	0.20	32.80	93.00	19.60	37.50	96.70	0.42	0.72	0.27	0.63	3	15.21	1.49	41.40	38.10	0.13	96.32
	3	0.00	9.30	0.80	0.00	0.10	47.80	0.40	0.40	0.20	36.20	95.30	15.00	36.40	98.90	0.30	0.66	0.42	0.66	3	27.73	1.70	31.68	37.00	0.23	98.35
	4	0.00	9.00	0.60	0.00	0.00	45.40	0.40	0.40	0.20	38.90	94.90	18.30	30.10	97.90	0.37	0.55	0.40	0.71	3	26.84	1.28	38.65	30.70	0.13	97.59
Fig. 2 (3)	1	0.00	0.60	1.00	0.00	0.00	50.80	0.30	0.60	0.30	44.70	98.30	38.10	14.10	99.70	0.81	0.27	0.08	0.85	3	1.79	2.13	80.47	14.70	0.02	99.10
	2	0.00	3.10	0.60	0.00	0.10	48.60	0.30	0.60	0.30	46.10	99.80	35.30	14.90	101.30	0.72	0.27	0.16	0.85	3	9.24	1.28	74.55	15.50	0.15	100.73
	3	0.00	1.70	0.90	0.00	0.00	49.30	0.30	0.70	0.30	46.40	99.70	37.70	13.00	101.00	0.78	0.24	0.12	0.87	3	5.07	1.91	79.62	13.60	0.05	100.26
	4	0.00	5.70	0.50	0.00	0.00	45.20	0.30	0.60	0.40	46.80	99.50	31.30	15.50	101.00	0.63	0.28	0.25	0.85	3	17.00	1.06	66.11	16.20	0.12	100.49
	5	0.00	5.60	0.60	0.00	0.00	45.60	0.20	0.60	0.40	47.30	100.30	32.00	15.10	101.90	0.64	0.27	0.25	0.85	3	16.70	1.28	67.58	15.70	0.06	101.32
Fig. 2 (4)	1	0.00	3.80	0.60	0.00	0.00	54.00	0.10	0.60	0.10	35.20	94.30	24.20	33.00	97.60	0.52	0.63	0.20	0.67	3	11.33	1.28	51.11	33.20	0.07	96.99
	2	0.00	7.10	1.10	0.00	0.00	44.60	0.10	0.40	0.00	43.00	96.40	24.90	21.90	98.60	0.51	0.40	0.31	0.79	3	21.17	2.34	52.59	22.00	0.05	98.15
Fig. 2 (5)	1	0.00	9.10	0.30	0.00	0.10	37.00	0.10	0.70	0.40	49.20	96.80	27.60	10.40	97.90	0.56	0.19	0.37	0.89	3	27.14	0.64	58.29	10.90	0.15	97.11
	2	0.00	9.80	0.40	0.00	0.10	36.50	0.10	0.70	0.30	49.90	97.90	27.00	10.60	98.90	0.54	0.19	0.39	0.89	3	29.22	0.85	57.02	11.00	0.10	98.19
	3	0.00	9.10	0.40	0.00	0.00	36.50	0.10	0.70	0.40	50.20	97.30	28.40	8.90	98.20	0.57	0.16	0.37	0.91	3	27.14	0.85	59.98	9.40	0.13	97.50
	4	0.00	9.80	0.40	0.00	0.00	35.30	0.10	0.60	0.30	51.10	97.50	28.00	8.00	98.30	0.56	0.14	0.39	0.92	3	29.22	0.85	59.14	8.40	0.10	97.71
	5	0.00	7.70	0.40	0.00	0.00	35.00	0.10	0.80	0.50	52.80	97.30	33.30	1.80	97.50	0.68	0.03	0.32	0.97	3	22.96	0.85	70.33	2.40	0.08	96.62
	6	0.00	12.00	0.50	0.00	0.10	31.90	0.10	0.50	0.20	53.00	98.30	25.80	6.90	98.90	0.50	0.12	0.45	0.93	3	35.78	1.06	54.49	7.20	0.21	98.75
	7	0.00	7.30	0.30	0.00	0.00	34.70	0.10	0.70	0.50	53.30	97.00	34.60	0.10	97.00	0.71	0.00	0.30	0.99	3	21.77	0.64	73.08	0.70	0.03	96.21
	8	0.00	7.70	0.30	0.00	0.00	34.20	0.10	0.60	0.30	53.80	97.10	34.20	0.00	97.10	0.70	0.00	0.31	0.99	3	22.96	0.64	72.23	0.40	0.29	96.52
Fig. 2 (6)	1	0.00	0.00	3.50	0.10	0.00	43.30	0.00	0.20	0.00	48.70	95.80	40.00	3.60	96.20	0.88	0.07	0.09	0.96	3	0.00	7.44	84.48	3.60	0.22	95.74
	2	0.00	0.10	5.00	0.00	0.00	41.40	0.00	0.30	0.00	49.50	96.20	39.30	2.30	96.40	0.86	0.05	0.12	0.97	3	0.30	10.63	83.00	2.30	0.09	96.32
	3	0.00	0.00	3.60	0.00	0.00	44.20	0.00	0.40	0.00	49.50	97.70	40.90	3.70	98.00	0.88	0.07	0.09	0.96	3	0.00	7.65	86.38	3.70	0.04	97.77
	4	0.00	0.00	3.30	0.00	0.10	43.90	0.00	0.30	0.00	49.50	97.20	41.10	3.10	97.50	0.89	0.06	0.08	0.97	3	0.00	7.02	86.80	3.10	0.10	97.02
	5	0.00	0.00	4.80	0.10	0.00	41.30	0.00	0.30	0.00	49.50	96.10	39.60	2.00	96.30	0.87	0.04	0.12	0.98	3	0.00	10.20	83.64	2.00	0.04	95.88
	6	0.00	0.00	3.40	0.00	0.10	43.50	0.00	0.40	0.00	49.50	97.00	41.00	2.80	97.20	0.89	0.06	0.09	0.97	3	0.00	7.23	86.59	2.80	0.07	96.69
	7	0.00	0.00	4.40	0.10	0.10	42.20	0.00	0.30	0.00	50.10	97.20	40.40	1.90	97.30	0.88	0.04	0.11	0.98	3	0.00	9.35	85.32	1.90	0.18	96.76
Fig. 3	1	0.00	0.00	3.60	0.10	0.10	47.10	0.00	0.60	0.00	44.80	96.30	36.40	11.90	97.50	0.79	0.23	0.10	0.88	3	0.00	7.65	76.88	11.90	0.20	96.63
	2	0.00	0.10	3.40	0.10	0.10	43.70	0.00	0.60	0.00	48.90	96.90	40.20	3.90	97.30	0.87	0.08	0.10	0.96	3	0.30	7.23	84.90	3.90	0.19	96.52
	3	0.00	0.00	4.20	0.00	0.00	43.00	0.00	0.50	0.10	48.80	96.70	39.50	3.90	97.10	0.86	0.08	0.11	0.96	3	0.00	8.93	83.42	4.00	0.06	96.41
	4	0.00	0.10	4.10	0.10	0.10	42.70	0.00	0.50	0.00	49.10	96.60	39.70	3.40	97.00	0.86	0.07	0.11	0.96	3	0.30	8.72	83.85	3.40	0.29	96.55
	5	0.00	0.10	4.40	0.20	0.00	43.10	0.00	0.50	0.00	49.20	97.60	39.50	4.10	98.00	0.85	0.08	0.12	0.96	3	0.30	9.35	83.42	4.10	0.27	97.45
	6	0.40	0.10	4.00	0.40	0.10	41.10	0.00	0.60	0.00	49.30	96.00	40.10	1.10	96.10	0.88	0.02	0.13	0.97	3	0.30	8.50	84.69	1.10	0.02	94.62
	7	0.00	0.00	4.30	0.00	0.00	42.00	0.00	0.50	0.00	49.40	96.30	40.10	2.20	96.50	0.88	0.04	0.11	0.97	3	0.00	9.14	84.69	2.20	0.05	96.08
	8	0.00	0.10	4.40	0.10	0.10	42.00	0.00	0.50	0.00	49.50	96.70	39.70	2.60	97.00	0.87	0.05	0.12	0.97	3	0.30	9.35	83.85	2.60	0.23	96.33
	9	0.00	0.10	3.80	0.00	0.20	41.40	0.00	0.60	0.00	49.50	95.50	40.50	1.00	95.60	0.89	0.02	0.10	0.98	3	0.30	8.08	85.54	1.00	0.15	95.07
	10	0.00	0.00	4.00	0.00	0.10	43.50	0.00	0.50	0.10	49.60	97.90	40.40	3.40	98.20	0.87	0.07	0.10	0.96	3	0.00	8.50	85.32	3.50	0.18	97.50
	11	0.00	0.00	3.90	0.00	0.10	42.90	0.00	0.60	0.30	50.00	97.80	40.80	2.30	98.10	0.88	0.04	0.11	0.97	3	0.00	8.29	86.17	2.60	0.22	97.29
	12	0.10	0.10	3.70	0.10	0.10	39.40	0.00	0.50	0.00	50.40	94.50	39.40	0.00	94.50	0.88	0.00	0.11	1.01	3	0.30	7.87	83.21	0.00	2.24	93.62
	13	0.30	0.10	3.20	0.10	0.00	39.50	0.00	0.60	0.00	50.60	94.30	39.50	0.00	94.30	0.88	0.00	0.10	1.02	3	0.30	6.80	83.42	0.00	3.01	93.53

TABLE II. CALCULATED DIFFERENT MINERAL COMPONENT FRACTIONS OF EACH ANALYZED SPOT OF OF THE RUTILO-ILMENITE EXSOLVED INTERGROWN GRAINS OF FIGURES 2, 3

Grain	Spot	SiO_2	MgO	MnO	CaO	ZnO	FeO	Al_2O_3	V_2O_3	Cr_2O_3	TiO_2	Total	Gek	Pyr	H	R	Total
Fig. 2 (1)	1	0.20	3.90	0.80	0.10	0.00	59.10	1.30	0.70	2.50	25.50	94.10	11.63	1.70	69.48	16.90	99.71
	5	0.00	2.00	0.30	0.00	0.00	30.10	0.10	0.50	0.30	63.00	96.40	6.09	0.64	33.86	58.59	99.18
	6	0.00	1.40	0.20	0.00	0.10	24.50	0.10	0.60	0.30	70.30	97.40	4.18	0.53	27.62	67.21	99.54
	7	0.00	0.80	0.20	0.00	0.00	19.30	0.10	0.50	0.30	75.00	96.40	2.42	0.43	21.91	73.22	97.97
Fig. 2 (2)	5	0.00	1.60	0.10	0.00	0.10	19.20	0.20	0.60	0.10	75.10	97.00	4.82	0.27	21.59	71.78	98.46
	6	0.00	0.50	0.10	0.10	0.00	7.30	0.00	0.80	0.10	88.50	97.40	1.56	0.2	8.23	87.41	97.4
Fig. 2 (3)	6	0.00	0.10	0.40	0.00	0.00	23.20	0.30	0.80	0.40	70.90	96.20	0.42	0.82	26.44	70.21	97.89
	7	0.00	0.70	0.30	0.00	0.00	19.50	0.20	0.70	0.20	75.40	97.20	2.17	0.6	22.11	73.69	98.56
Fig. 2 (4)	3	0.00	1.50	0.30	0.00	0.00	25.20	0.00	0.60	0.00	68.20	95.90	4.38	0.71	28.07	64.91	98.07
	4	0.00	0.70	0.10	0.00	0.00	17.20	0.00	0.70	0.10	78.80	97.60	2.17	0.14	19.16	77.33	98.8
	5	0.00	0.00	0.10	0.00	0.00	1.20	0.00	0.60	0.00	96.30	98.20	0.05	0.12	1.37	96.18	97.72
	6	0.00	0.00	0.00	0.00	0.10	1.20	0.00	0.70	0.00	96.60	98.60	0.05	0.02	1.34	96.54	97.95
Fig. 2 (5)	9	0.00	5.60	0.20	0.00	0.00	21.80	0.10	0.70	0.20	68.70	97.30	16.55	0.48	24.53	57.5	99.07
	10	0.00	4.80	0.20	0.00	0.00	20.60	0.00	0.80	0.30	71.20	97.90	14.24	0.36	23.24	61.61	99.45
	11	0.00	4.10	0.30	0.00	0.00	19.00	0.00	0.80	0.30	73.00	97.50	12.27	0.57	21.38	64.54	98.76
	12	0.00	4.10	0.20	0.00	0.00	18.50	0.10	0.80	0.20	73.70	97.60	12.11	0.52	20.81	65.43	98.87
	13	0.00	2.80	0.10	0.00	0.10	16.40	0.00	0.80	0.20	77.40	97.80	8.25	0.25	18.48	71.77	98.76
	14	0.00	3.60	0.20	0.00	0.00	15.70	0.00	0.80	0.20	77.70	98.20	10.65	0.33	17.66	70.5	99.14
	15	0.00	3.10	0.20	0.00	0.10	12.90	0.00	0.80	0.10	80.60	97.80	9.17	0.37	14.53	74.33	98.39
Fig. 2 (6)	8	0.00	0.00	0.10	0.00	0.00	25.40	0.00	0.50	0.00	69.80	95.90	0.12	0.28	28.23	69.57	98.2
	9	0.20	0.20	0.20	0.20	0.00	16.30	0.50	0.50	0.00	72.10	90.10	0.45	0.49	18.57	71.54	91.05
	10	0.00	0.10	0.10	0.00	0.00	6.10	0.00	0.60	0.00	91.80	98.80	0.17	0.21	6.85	91.62	98.85
	11	0.00	0.00	0.10	0.00	0.10	5.30	0.00	0.70	0.00	93.50	99.70	0.1	0.11	5.95	93.34	99.5
Fig. 3	14	0.00	0.10	0.10	0.00	0.00	23.30	0.00	1.10	0.10	71.90	96.50	0.21	0.21	25.96	71.62	98
	15	1.20	0.20	0.20	0.90	0.10	7.20	1.00	1.00	0.00	80.40	92.20	0.69	0.47	9	79.7	89.86
	16	1.80	0.40	0.20	1.20	0.00	6.10	1.40	1.00	0.00	81.20	93.40	1.19	0.41	8.22	80.19	90.02
	17	0.40	0.30	0.10	0.40	0.00	9.70	1.20	1.10	0.00	81.30	94.50	0.8	0.27	11.94	80.61	93.63
	18	0.00	0.10	0.00	0.00	0.00	12.10	0.00	0.90	0.10	83.20	96.50	0.26	0.07	13.53	83.02	96.88
	19	1.40	0.30	0.20	1.00	0.00	4.10	1.20	1.10	0.00	83.60	92.70	0.84	0.36	5.69	82.84	89.73
	20	0.10	0.10	0.00	0.20	0.00	9.50	0.10	1.00	0.00	85.50	96.50	0.43	0.06	10.6	85.23	96.32
	21	0.00	0.10	0.10	0.20	0.00	9.20	0.00	0.90	0.00	86.40	96.80	0.17	0.11	10.28	86.26	96.83
	22	0.00	0.10	0.00	0.00	0.00	9.60	0.00	0.90	0.00	86.70	97.50	0.29	0.09	10.75	86.46	97.58
	23	0.00	0.10	0.10	0.10	0.10	6.90	0.10	1.10	0.00	88.70	97.10	0.2	0.16	7.73	88.5	96.59
	24	0.10	0.10	0.00	0.10	0.00	6.60	0.00	1.00	0.00	89.00	96.90	0.27	0.08	7.32	88.76	96.42
	25	0.00	0.10	0.00	0.00	0.00	5.80	0.00	0.90	0.00	90.70	97.60	0.4	0.07	6.43	90.38	97.28
	26	0.00	0.00	0.10	0.10	0.00	4.10	0.00	1.00	0.00	90.80	96.10	0.12	0.14	4.59	90.67	95.53
	27	0.10	0.00	0.10	0.10	0.00	5.10	0.20	1.10	0.10	91.20	97.90	0.11	0.22	5.91	90.97	97.21
	28	0.00	0.10	0.10	0.10	0.00	4.70	0.00	0.90	0.00	91.40	97.30	0.29	0.14	5.24	91.14	96.81
	29	0.00	0.00	0.10	0.10	0.00	4.80	0.00	1.00	0.00	92.30	98.20	0.07	0.13	5.32	92.15	97.66
	30	0.00	0.00	0.00	0.10	0.00	3.90	0.00	0.90	0.00	93.20	98.10	0.13	0.03	4.36	93.1	97.62
	31	0.00	0.00	0.10	0.00	0.00	3.40	0.00	0.90	0.10	93.60	98.10	0.06	0.13	3.79	93.48	97.46

TABLE III. ORIGINAL MICROPROBE CHEMICAL ANALYSIS OF SOME SPOTS OF GRAINS FROM FIGURES 2, 3

Grains	Spots	SiO_2	MgO	MnO	CaO	ZnO	FeO	Al_2O_3	V_2O_3	Cr_2O_3	TiO_2	Total
Fig. 2(2)	1	46.36	7.92	0.20	10.20	0.01	13.55	11.23	0.11	0.00	4.62	94.21
Fig. 3	32	23.65	18.77	0.14	0.66	0.03	15.91	17.12	0.26	0.03	13.96	90.53
	33	7.24	0.82	0.36	1.21	0.04	16.44	2.59	0.71	0.13	41.55	71.10
	34	7.77	1.41	0.85	1.25	0.02	15.35	3.75	0.54	0.06	43.36	74.36
	35	1.02	0.24	1.02	0.75	0.00	18.48	0.73	0.57	0.48	46.78	70.06
	36	3.63	0.85	0.28	1.51	0.00	14.80	2.04	0.67	0.03	47.65	71.45
	37	7.70	0.68	0.32	3.50	0.12	9.95	2.22	0.57	0.08	50.96	76.09
	38	4.96	0.90	0.55	2.17	0.00	10.43	1.64	0.60	0.02	52.53	73.80
	39	7.29	1.00	0.18	0.63	0.03	5.69	3.64	0.71	0.01	56.14	75.31

Spot 1 of grain 2 of Figure 2 (Table III) is a definite silicate mineral composed of Fe, Ca, Mg, Ti, and Al-silicate. Spots 2-4 (Figure 2, Table I), are mixtures of several mineral components. Using the same method of calculation with (M1), the various mineral components of spots 2- 4 of grain (2) are: Spot 2: 41.40% ilmenite, 38.10% hematite, 15.21% geikielite, 1.49% pyrophanite, and 0.13% rutile. Spot 3: 31.68% ilmenite, 37% hematite, 27.73% geikielite, 1.70% pyrophanite, and 0.23% rutile. Spot 4: 38.65% ilmenite, 30.70% hematite, 26.84% geikielite, 1.28% pyrophanite, and 0.13% rutile. It is obvious that the ilmenite component in these spots is partially altered into hematite and the detected exsolved rutile bodies. It is obvious that the lightness of spot area is determined according to the amount of hematite component. As the hematite % increases, the lightness increases (spots 2 and 3), and vice versa (spot 4).

Spots 5 and 6 of grain (2) of Figure 2 (Table II) are ferriferous rutile composed mostly of rutile with considerable amounts of hematite in solid solution, ranging between 8.23 and 21.59%. Using the M3 method of calculation, the mineral components for each of the two spots are: Spot 5: 21.59% hematite, 4.82% geikielite, 0.27% pyrophanite, and 71.78% rutile and spot 6: 8.23% hematite, 1.56% geikielite 0.20%, pyrophanite, and 87.41% rutile. Spots 1-5 of grain (3) of Figure 2 (Table I) are ferriilmenite with Fe_2O_3 content ranging between 13.60 and 16.20%. Both spots 6-7 of Figure 2 are ferriferous rutile (Table II).

Spots 1 and 2 of grain (4) of Figure 2 are ferriilmenite (Table I), spots 3 and 4 are ferriferous rutile, and spots 5 and 6 are rutile with minor Fe_2O_3 content (Table II). Using the M1 method of calculation, the mineral components of spots 1 and 2 are: Spot 1: 51.11% ilmenite, 33.20% hematite, 11.33% geikielite, 1.28% pyrophanite, and 0.07% rutile. Spot 2: 52.59% ilmenite, 22%, hematite, 21.17% geikielite, 2.34% pyrophanite, and 0.05% rutile. These two spots are solid solutions of ilmenite, hematite, geikielite, pyrophanite, and traces of rutile. It is obvious that both Mg and Mn follow FeO and not Fe_2O_3, hence as the content of hematite decreases, as the content of geikielite and/or pyrophanite increases. Geikielite and pyrophanite are mixed easier with ilmenite than with hematite. Spots 3 and 4 are rutile mixed with hematite, ranging between 19.16 and 28.07%.

Spots 5 and 6 are mostly rutile with minor hematite, which ranges between 1.34 and 1.37%. It is obvious that the relatively larger and darker rutile exsolved intergrowths are composed mostly of rutile (more than 95% TiO_2), while the relatively smaller ones are mainly ferriforous rutile with considerable amounts of mixed hematite (Figure 2, Table II). Spots 1-6 of grain (5) of Figure 2 are ferriilmenite, 7 and 8 are ilmenite (Table I). All the iron of spot 8 is ferrous iron. It is obvious that most of ferriilmenite containing exsolved intergrowths of rutile contain a considerable amount of MgO as geikielite. Spots 9-15 are ferriferous rutile mixed with hematite, geikielite, and pyrophanite in solid solution (Table II). Using the same method of calculations of (2) and (3) grains, and converting all analyzed iron as FeO to Fe_2O_3 to be calculated as hematite, the mineral components composed for each spot are shown in Table II. Spots 1-7 of grain (6) of Figure 2 (Table I) are ferriilmenite with Fe_2O_3 content ranging between 1.9 and 3.7%. Spots 10 and 11 are ferriferous rutile. Spots 8 and 9 are ilmenite altered to rutile and hematite (Table II). Spot 9 is located beside the edge of the grain. The activity of water seems to be relatively greater hence a partial leaching of hematite component occurred. The total oxide sum of this spot is 91.05%, which reflects the existence of molecular water (Table II).

Spots 1-13 of the grain of Figure 3 (Table I) are composed mainly of ilmenite and pyrophanite with minor amounts of hematite and other mineral components. Spots from 1 to 11, are ferriilmenite with Fe_2O_3 content ranging between 1 and 11.90%. Spots 12 and 13 are ilmenite, in which most of the mixed Fe_2O_3 is leached out. All the iron content is ferrous iron. Some molecular water is included in these two spots. The analyzed total oxide sum of the two spots is 94.3 and 94.5% respectively (Table I).

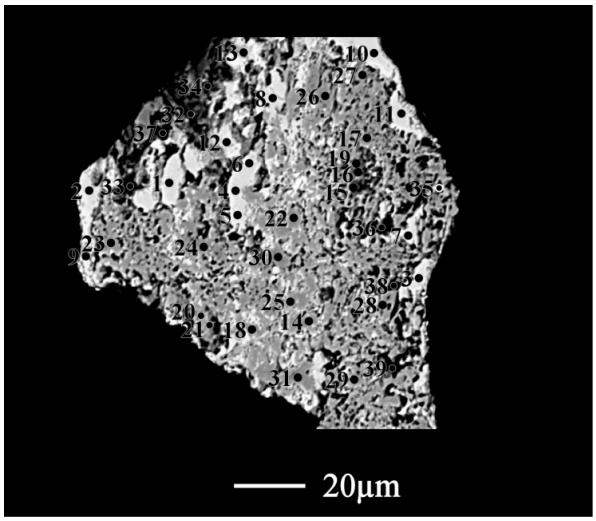

Fig. 3. BSE image of a composite ilmenite grain. Spots 1-13 are composed of ilmenite enriched with MnO content. Spots 14-31 are ilmenite altered to rutile and hematite, and spots 32-39 are alterations of a definite silicate mineral.

Spots 14-31 are ilmenite altered to rutile and hematite. They are composed mainly of rutile and hematite mineral components (Table II). Spots 15, 16, and 19 are in the neighborhood of voids where the activity of molecular water is relatively higher. Spots 32-39 are an alteration of a definite silicate mineral, Mg Fe Al-silicate, attached with ilmenite altered to rutile and hematite (Table III). The hematite component is partially leached leaving the remaining rutile associated with the products of the altered silicate mineral. Most of these last spots contain molecular and/or structural water.

B. Titanhematite (4.4%)

Authors in [26] explained that hematite is not so widely distributed in magmatic rocks, as it is known from the literature. Authors in [27] showed that hematite is almost wholly Fe_2O_3 and subtitanhematite is Fe_2O_3 with 1.5 to 5% TiO_2 as $FeO.TiO_2$ or TiO_2 or both while titanhematite is Fe_2O_3 with 5-10% TiO_2 as $FeO.TiO_2$ up to about 13% plus excess TiO_2 up to about 3% in solid solution. Titanhematite or white ilmenite is hematite containing a maximum of 10% $FeTiO_3$ in solid solution. If the $FeTiO_3$-content exceeds 10%, oriented intergrowths of ilmenite and Ti-hematite may be formed [28]. A number of fabrics in which the titanhematite is considered as the major component (the host mineral) have been observed. These include the following arranged in decreasing order of abundance:

1) Ilmenite-Hematite Exsolution Intergrowth

The intergrowth was called ilmenohematite where micro intergrowths of ferrianilmenite or hemoilmenite are enclosed in the titanhematite host [27]. Although ferriilmenite exsolution bodies are found in two different sizes in the host titanlrematite, they cannot be considered as two distinct generations. Many of

the relatively larger ferriilmenite exsolution lamellae are observed to have coalesced, are frequently irregular, and seem to grade into smaller bodies. So, the ferriilmenite-titanhematite intergrowth may be interpreted as a result of unmixing of an original ilmenite-hematite solid solution and most of the relatively larger ferriilmenite exsolution lamellae that seem to have grown in situ by diffusion.

2) Rutile-Hematite Exsolution Intergrowth

Such intergrowth is called as rutilohematite where microintergrowths of rutile or exsolved rutile grains are enclosed in the titanhematite host [27]. A few exsolved rutile needles cut the host titanhematite grains from side to side, suggesting that most of them represent the unmixing of excess TiO_2 originally dissolved in the Fe_2O_3 solid solution. The same intergrowth was observed in [29] in metamorphosed beach sands.

3) Rutile-Ilmenite-Hematite Exsolution Intergrowth

This intergrowth was called as ilmenorutilohematite where exsolved micro intergrowths of ferrianilmenite or hemoilmenite and rutile are enclosed in the host titanhematite [27]. Such type of exsolved intergrowth was observed in the sands of Lake Oulu, Finland [30]. The exsolved ferriilmenite lamellae had short, more spindle-shaped bodies parallel to the (0001) plane of titanhematite while the exsolved rutile needles were common in at least 6 directions. Authors in [29] recorded the same type of intergrowth, but the exsolved rutile lamellae were found in the typical Blitz texture. Authors in [31] believed that the rutile lamellae are of an earlier generation than the ferriilmenite exsolution bodies. However, authors in [25] concluded that the unmixing of the ilmenite-hematite solid solution to ferriilmenite and titanhematite started before the separation of the excess TiO_2 as rutile. Authors in [14] agreed with this conclusion, since the rutile lamellae are observed to cut the ferriilmenite exsolutions, i.e. they are, therefore, of later origin. On the other hand, authors in [32] explained the development of the rutile exsolutions as a result of the partial oxidation (under high oxidation potential) of $FeTiO_3$ in a mixed crystal lying near the Fe_2O_3-$FeTiO_3$ join, on the TiO_2 side of the system FeO-Fe_2O_3-TiO_2 to hematite and rutile:

$$2\ FeTiO_3 + O \rightarrow Fe_2O_3 + 2\ TiO_2$$

The resulting rutile is then dissolved at sufficient temperatures in the $FeTiO_3$-Fe_2O_3 solid solution (especially on the Fe_2O_3 side). Later unmixing of the rutile in solid solution takes place. We believe that the exsolved rutile lamellae are of later origin and are the result of the unmixing of the excess TiO_2, originally dissolved in the $FeTiO_3$-Fe_2O_3 solid solution. The frequency of these exsolved rutile lamellae is very low compared with the exsolved ferriilmenite lamellae and some of them were detected to cut the ferriilmenite exsolutions.

The microprobe findings of some titanhematite grains of different fabrics are: In grain (1), all the analyzed 6 spots of Figure 4 (Tables IV, V) are mainly Fe_2O_3 with only minor portions of TiO_2. The grain is most probably hematite. In grain (2), the analyzed 5 spots (Figure 4, Tables IV, V) are composed of hematite. The V_2O_3 content ranges between 0.18 and 0.2%. Spots 1-4 of grain (3), (Figure 4, Tables IV, V) are hematite with minor TiO_2. The V_2O_3 content of these spots ensures that V_2O_3 follows Fe_2O_3 rather than FeO. Also, the negligible content of MgO and MnO ensures that these two oxides do not follow Fe_2O_3. Spot 5 is silica which is recorded along the edges of grain (3), (Figure 4, Table VIII). This may reflect the ability of silica to replace Fe_2O_3. Spots 6-7 are calcite, where the remaining percentage of each spot is detected to be carbon (Figure 4, Table VIII).

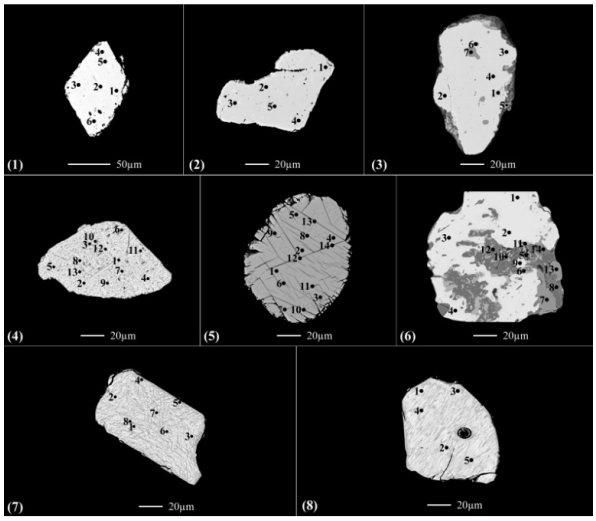

Fig. 4. BSE images of various titanhematite exsolved intergrown grains.

Spots 1 and 2 of grain (4) of Figure 4 (Tables IV, V) are ilmenite. Spot 3 is hematite altered to goethite. Spots 4-13 are hematite altered to goethite where the analyzed total oxide sum decreases by about one tenth of the analyzed value of Fe_2O_3 content which corresponds the content of structural water (OH^-) necessary for converting hematite to goethite (FeOOH), (Figure 4, Tables IV, V). In these spots, V_2O_3 content ranges between 0.69 and 0.78%. It follows Fe_2O_3, which ranges between 87.06 and 89.99%. TiO_2 content ranges between 0.81 and 1.22%. Spots 1-5 of grain (5) of Figure 4 (Tables IV, V) are titanhematite. MgO and MnO contents range between 0.06 and 0.09% and 0.16 and 0.28% respectively. TiO_2 content ranges between 8.29 and 9.15%, while the FeO content ranges between 6.99 and 7.83%. The recorded TiO_2 content seems to be related to the contained ilmenite. Spots 6-14 have total oxide sum ranging between 93.2 and 96.77%. TiO_2 content ranges between 24.05 and 45.73%, while the Fe_2O_3 content ranges between 50.59 and 5.78%. At spot 6, the TiO_2 content is 24.05% while the Fe_2O_3 content is 50.59%. On the other hand, at spot 14, the TiO_2 content is 45.73%, while the Fe_2O_3 content is 5.78%. There is an obvious reverse relation between TiO_2 and Fe_2O_3 inside each spot. Also, it is noticed that although the spots 12, 14 are located at the same exsolved intergrowth lamella, they have widely varying contents of TiO_2 and Fe_2O_3, while the analyzed total oxide sum is almost the same: 93.67 and 93.20% respectively. Also, the MnO and MgO contents are negligible which may indicate the absence of ferrous iron. In fact, spots 6-14 are ilmenite alteration mixtures of rutile and hematite or some of spots are pseudobrookite of the Fe_2TiO_5

type, mixed with an individual TiO_2 phase, most probably rutile, and maybe also Fe_2O_3.

In grain (6) of Figure 4 (Tables IV, V), spots 1-6 are titanhematite. The FeO content ranges between 1.9 and 7.86% which corresponds to the analyzed content of TiO_2: 2.17-8.82%, indicating the content of ilmenite. Spots 7-13 do not give acceptable results using the ilmenite program (Figure 4, Table VIII). Spots 7-8 are made from a CaFeAl-silicate mineral. The area of spot 8 is darker than that of spot 7 due to the alteration of the silicate mineral and an enrichment of the content of SiO_2 (Table VIII). Spot 13 is silica. In spots 9-12 of grain (6), the silica ranges between 5.57 and 90.85%, while TiO_2 ranges between 94.98 and 8.51%. It is obvious that the titanhematite of spot 9 is replaced by SiO_2, while the contained TiO_2 remained. Spots 10-12 are most probably rutilo-hematite (spots 10, 11), or ferriforous rutile (spot 12), where Fe_2O_3 is replaced by SiO_2. The analyzed total oxide sum of some spots may be greater than 100%, due to the irregularity and the voids of the measured spot surface.

In grain (7) of Figure 4 (Tables IV, V), spots 1-3 may be the result of high temperature alteration of ilmeno-hematite fabric, producing a mixture of hematite and rutile in solid solution. Spots 4-8 do not give acceptable results using the ilmenite program (Table V). These spots have TiO_2 content ranging between 62.23 and 82.42%. By converting the analyzed FeO content into Fe_2O_3, the obtained values range between 15.22 and 34.83% and the corresponding total oxide sum of these spots ranges between 98.03 and 98.94%, respectively (Table V). There is a distinct reverse relation between TiO_2 and Fe_2O_3 at these spots. These spots are most probably pseudorutile or mixtures of rutile and hematite obtained by the alteration of contained ilmenite exsolved intergrowth.

In grain (8), spots 1-2 (Figure 4, Tables IV, V) are hematite and rutile in solid solution. Spots 3-6 do not give acceptable results using the ilmenite program. Spots 3-5 have TiO_2 content ranging between 63.66 and 64.72%. By converting the analyzed FeO content into Fe_2O_3, the obtained values range between 25.94 and 33.24% (Table VIII). These spots are ferriforous rutile or pseudorutile obtained by the alteration of contained ilmenite exsolved intergrowth, as the last grain (7). Spot 6 is a definite silicate mineral (Table VIII) MgFeAl-silicate, with some of contained structural and/or molecular water.

4) Ferromagnetic Titanhematite

All the analyzed 6 grains (Figure 5, Tables VI, VII), are separated within the ferromagnetic fraction associated with magnetite and titanomagnetite grains. They are not contained within the final bulk ilmenite concentrate. In these grains, spot 5 of (4), spots 1-5 and 11 of (5), and spots 13, 14 of (6) do not give acceptable results. The other investigated spots (Figure 5, Tables VI, VII), of the grains are:

Grain (1): Spots 1-6 are martitized magnetite. In spot 1, the recorded contents of SiO_2, MgO, CaO, and Al_2O_3 may be remnants of altered silicate mineral inclusions.

Grain (2): Spots 1, 2 are hematite while spots 3, 4 are remnants of magnetite.

Grain (3): Spots 1-5 (Figure 5) are titanomagnetite with TiO_2 content ranging between 13.67 and 17.03%. Spots 6-11 are titanhematite with TiO_2 content ranging between 22.93 and 26.5%. Spots 12, 13 are most probably pseudobrookite (Table VIII), while spot 14 is ferriilmenite.

Grain (4): Spots 1, 2 are pseudobrookite, while spot 5 is calcite (Table VIII). Spots 3, 4 are titanhematite after titanomagnetite.

Grain (5): Spots 1-5 are rutile (Table VII). Spots 6-8 are martitized titanomagnetite with TiO_2 content ranging between 8.77 and 9.55%. Spots 9, 10 are martitized titanomagnetite with relatively higher content of TiO_2, which ranges between 17.8 and 19.54%. Spot 11 is martitized titanomagnetite into titanhematite and most of Fe_2O_3 content is leached (Table VIII). The recorded SiO_2 and Al_2O_3 are due to the increased water activity during the alteration and leaching of titanhematite.

Grain (6): Spots 1-9 are martitized titanomagnetite with TiO_2 content ranging between 13.43 and 24.37% (Tables VI, VII). Spots 10-12 are ilmenite (Tables VI, VII), spot 13 is leached ilmenite, and spot 14 is calcite (Table VIII).

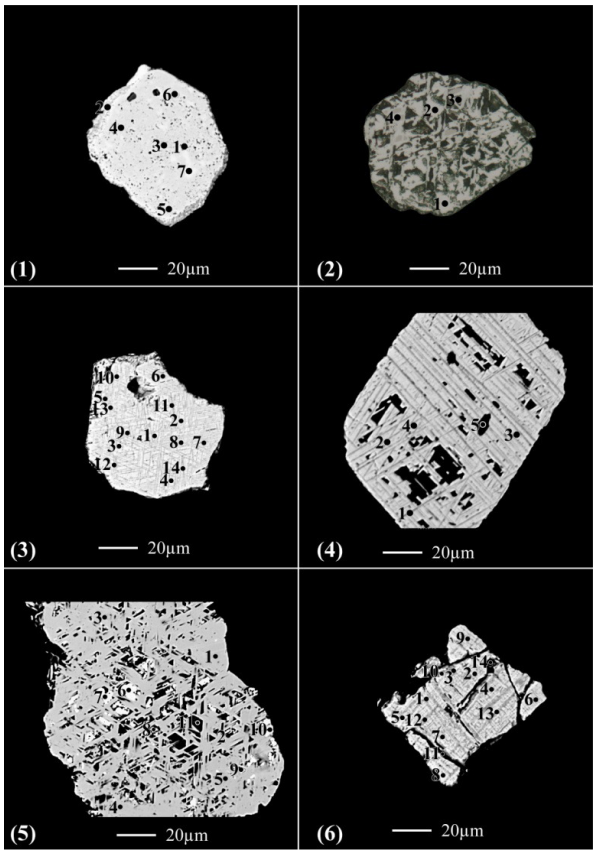

Fig. 5. BSE images of various ferromagnetic titanhematite grains. They are most probably produced by the process of martitization after titanomagnetite.

TABLE IV. MICROPROBE CHEMICAL ANALYSIS AND MOLECULAR FORMULAE OF THE ANALYZED SPOTS OF THE VARIOUS TITANHEMATITE EXSOLVED INTERGROWN GRAINS OF FIGURE 4

Grain	Spot	SiO_2	MgO	MnO	CaO	ZnO	FeO	Al_2O_3	V_2O_3	Cr_2O_3	TiO_2	Total	SiO_2	MgO	MnO	CaO	ZnO	FeO	Fe_2O_3	Al_2O_3	V_2O_3	Cr_2O_3	TiO_2	Total	Ferrous Fe	Ferric Fe	Other cations	Ti	O
Fig. 4 (1)	1	0.08	0.00	0.00	0.00	0.00	88.88	0.00	0.03	0.02	0.35	89.36	0.08	0.00	0.00	0.00	0.00	0.40	98.29	0.00	0.03	0.02	0.35	99.18	0.01	1.98	0.01	0.01	3
	2	0.00	0.00	0.06	0.01	0.00	88.89	0.00	0.04	0.06	0.14	89.18	0.00	0.00	0.06	0.01	0.00	0.05	98.70	0.00	0.04	0.06	0.14	99.04	0.00	1.99	0.01	0.00	3
	3	0.00	0.01	0.05	0.01	0.01	88.89	0.00	0.06	0.00	0.23	89.27	0.00	0.01	0.05	0.01	0.01	0.11	98.64	0.00	0.06	0.00	0.23	99.12	0.00	1.99	0.01	0.00	3
	4	0.10	0.02	0.00	0.01	0.00	89.27	0.00	0.07	0.01	0.24	89.71	0.10	0.02	0.00	0.01	0.00	0.28	98.86	0.00	0.07	0.01	0.24	99.59	0.01	1.98	0.01	0.00	3
	5	0.00	0.03	0.03	0.06	0.00	89.41	0.00	0.03	0.06	0.26	89.88	0.00	0.03	0.03	0.06	0.00	0.08	99.25	0.00	0.03	0.06	0.26	99.80	0.00	1.99	0.01	0.01	3
	6	0.00	0.00	0.07	0.00	0.00	91.23	0.00	0.02	0.05	0.33	91.70	0.00	0.00	0.07	0.00	0.00	0.22	101.11	0.00	0.02	0.05	0.33	101.80	0.00	1.99	0.00	0.01	3
Fig. 4 (2)	1	0.00	0.00	0.03	0.00	0.05	87.74	0.00	0.20	0.00	0.17	88.19	0.00	0.00	0.03	0.00	0.05	0.07	97.40	0.00	0.20	0.00	0.17	97.92	0.00	1.99	0.01	0.00	3
	2	0.00	0.00	0.00	0.00	0.04	88.34	0.01	0.19	0.04	0.17	88.78	0.00	0.00	0.00	0.00	0.04	0.12	98.01	0.01	0.19	0.04	0.17	98.57	0.00	1.99	0.01	0.00	3
	3	0.00	0.01	0.03	0.02	0.00	88.53	0.00	0.18	0.04	0.42	89.23	0.00	0.01	0.03	0.02	0.00	0.31	98.01	0.00	0.18	0.04	0.42	99.02	0.01	1.98	0.01	0.01	3
	4	0.00	0.00	0.07	0.00	0.00	89.05	0.00	0.19	0.02	0.42	89.76	0.00	0.00	0.07	0.00	0.00	0.31	98.60	0.00	0.19	0.02	0.42	99.61	0.01	1.98	0.01	0.01	3
	5	0.02	0.00	0.04	0.02	0.04	90.03	0.00	0.20	0.03	0.35	90.72	0.02	0.00	0.04	0.02	0.04	0.23	99.76	0.00	0.20	0.03	0.35	100.68	0.01	1.98	0.01	0.01	3
Fig. 4 (3)	1	0.33	0.24	0.04	0.09	0.00	86.44	0.30	0.36	0.12	1.49	89.43	0.33	0.24	0.04	0.09	0.00	1.14	94.77	0.30	0.36	0.12	1.49	98.90	0.03	1.90	0.06	0.03	3
	2	0.00	0.01	0.07	0.04	0.14	87.04	0.01	0.31	0.03	1.22	88.87	0.00	0.01	0.07	0.04	0.14	0.85	95.76	0.01	0.31	0.03	1.22	98.43	0.02	1.94	0.02	0.02	3
	3	0.02	0.01	0.04	0.04	0.05	87.39	0.03	0.31	0.05	1.20	89.14	0.02	0.01	0.04	0.04	0.05	0.95	96.03	0.03	0.31	0.05	1.20	98.73	0.02	1.94	0.02	0.02	3
	4	0.02	0.00	0.07	0.04	0.00	87.56	0.03	0.34	0.06	0.99	89.11	0.02	0.00	0.07	0.04	0.00	0.81	96.39	0.03	0.34	0.06	0.99	98.74	0.02	1.95	0.02	0.02	3
Fig. 4 (4)	1	0.00	0.05	2.77	0.03	0.07	42.44	0.00	0.41	0.05	49.90	95.71	0.00	0.05	2.77	0.03	0.07	41.90	0.60	0.00	0.41	0.05	49.90	95.77	0.92	0.01	0.08	0.99	3
	2	0.03	0.07	2.88	0.00	0.00	43.09	0.00	0.37	0.03	49.87	96.35	0.03	0.07	2.88	0.00	0.00	41.86	1.37	0.00	0.37	0.03	49.87	96.49	0.92	0.03	0.08	0.98	3
	3	5.64	0.96	0.06	0.11	0.00	73.79	0.84	0.77	0.08	0.86	83.10	5.64	0.96	0.06	0.11	0.00	5.60	75.75	0.84	0.77	0.08	0.86	90.67	0.13	1.60	0.34	0.02	3
	4	0.20	0.05	0.02	0.04	0.00	79.32	0.02	0.74	0.08	0.97	81.44	0.20	0.05	0.02	0.04	0.00	0.96	87.06	0.02	0.74	0.08	0.97	90.14	0.02	1.93	0.04	0.02	3
	5	0.16	0.02	0.02	0.06	0.00	79.63	0.04	0.78	0.11	0.94	81.75	0.16	0.02	0.02	0.06	0.00	0.90	87.46	0.04	0.78	0.11	0.94	90.49	0.02	1.93	0.04	0.02	3
	6	0.16	0.04	0.04	0.07	0.07	79.73	0.07	0.72	0.05	1.22	82.15	0.16	0.04	0.04	0.07	0.07	1.04	87.43	0.07	0.72	0.05	1.22	90.89	0.03	1.92	0.05	0.03	3
	7	0.24	0.06	0.00	0.04	0.00	80.37	0.08	0.70	0.03	0.81	82.31	0.24	0.06	0.00	0.04	0.00	0.86	88.33	0.08	0.70	0.03	0.81	91.13	0.02	1.93	0.04	0.02	3
	8	0.31	0.06	0.06	0.07	0.03	80.84	0.09	0.78	0.03	0.81	83.06	0.31	0.06	0.06	0.07	0.03	0.82	88.91	0.09	0.78	0.03	0.81	91.94	0.02	1.93	0.05	0.02	3
	9	0.12	0.02	0.05	0.06	0.00	80.94	0.07	0.75	0.08	0.82	82.90	0.12	0.02	0.05	0.06	0.00	0.72	89.12	0.07	0.75	0.08	0.82	91.80	0.02	1.94	0.04	0.02	3
	10	0.21	0.02	0.02	0.05	0.08	80.98	0.09	0.69	0.06	0.98	83.19	0.21	0.02	0.02	0.05	0.08	0.95	88.91	0.09	0.69	0.06	0.98	92.07	0.02	1.92	0.05	0.02	3
	11	0.21	0.01	0.00	0.06	0.04	81.18	0.04	0.69	0.04	1.12	83.39	0.21	0.01	0.00	0.06	0.04	1.13	88.94	0.04	0.69	0.04	1.12	92.28	0.03	1.92	0.04	0.02	3
	12	0.14	0.04	0.01	0.04	0.00	81.60	0.05	0.73	0.08	0.83	83.51	0.14	0.04	0.01	0.04	0.00	0.80	89.77	0.05	0.73	0.08	0.83	92.48	0.02	1.94	0.04	0.02	3
	13	0.20	0.04	0.08	0.06	0.00	81.83	0.05	0.74	0.08	0.91	84.00	0.20	0.04	0.08	0.06	0.00	0.83	89.99	0.05	0.74	0.08	0.91	92.99	0.02	1.93	0.05	0.02	3
Fig. 4 (5)	1	0.00	0.09	0.22	0.02	0.07	80.70	0.06	0.28	0.12	8.29	89.85	0.00	0.09	0.22	0.02	0.07	6.99	81.89	0.06	0.28	0.12	8.29	98.03	0.16	1.65	0.03	0.17	3
	2	0.00	0.06	0.16	0.01	0.05	80.97	0.03	0.33	0.09	8.53	90.22	0.00	0.06	0.16	0.01	0.05	7.35	81.79	0.03	0.33	0.09	8.53	98.40	0.16	1.65	0.02	0.17	3
	3	0.00	0.09	0.28	0.00	0.07	80.69	0.05	0.33	0.10	8.61	90.20	0.00	0.09	0.28	0.00	0.07	7.24	81.60	0.05	0.33	0.10	8.61	98.35	0.16	1.64	0.03	0.17	3
	4	0.00	0.09	0.17	0.01	0.04	81.00	0.07	0.29	0.06	8.78	90.50	0.00	0.09	0.17	0.01	0.04	7.52	81.63	0.07	0.29	0.06	8.78	98.66	0.17	1.64	0.02	0.18	3
	5	0.00	0.09	0.20	0.00	0.05	80.38	0.06	0.28	0.05	9.15	90.25	0.00	0.09	0.20	0.00	0.05	7.83	80.60	0.06	0.28	0.05	9.15	98.31	0.18	1.62	0.02	0.18	3
	6	0.01	0.04	0.09	0.00	0.01	67.02	0.04	0.29	0.06	24.05	91.60	0.01	0.04	0.09	0.00	0.01	21.48	50.59	0.04	0.29	0.06	24.05	96.66	0.48	1.02	0.02	0.49	3
	7	0.00	0.01	0.11	0.01	0.00	66.36	0.02	0.37	0.09	24.90	91.88	0.00	0.01	0.11	0.01	0.00	22.25	49.01	0.02	0.37	0.09	24.90	96.77	0.50	0.99	0.02	0.50	3
	8	0.00	0.04	0.08	0.00	0.00	62.34	0.03	0.43	0.05	28.10	91.07	0.00	0.04	0.08	0.00	0.00	25.13	41.34	0.03	0.43	0.05	28.10	95.20	0.57	0.84	0.02	0.57	3
	9	0.00	0.01	0.07	0.00	0.00	60.87	0.02	0.44	0.09	29.28	90.77	0.00	0.01	0.07	0.00	0.00	26.27	38.44	0.02	0.44	0.09	29.28	94.61	0.60	0.79	0.02	0.60	3
	10	0.00	0.01	0.05	0.01	0.01	59.09	0.04	0.39	0.11	30.96	90.66	0.00	0.01	0.05	0.01	0.01	27.77	34.80	0.04	0.39	0.11	30.96	94.14	0.63	0.72	0.02	0.64	3
	11	0.00	0.00	0.08	0.01	0.01	55.15	0.04	0.39	0.08	35.16	90.93	0.00	0.00	0.08	0.01	0.01	31.53	26.25	0.04	0.39	0.08	35.16	93.55	0.72	0.54	0.02	0.72	3
	12	0.00	0.00	0.07	0.00	0.03	53.60	0.04	0.48	0.07	37.13	91.42	0.00	0.00	0.07	0.00	0.03	33.31	22.55	0.04	0.48	0.07	37.13	93.67	0.76	0.46	0.02	0.76	3
	13	0.00	0.02	0.04	0.01	0.00	50.91	0.01	0.45	0.06	42.49	93.99	0.00	0.02	0.04	0.01	0.00	38.13	14.19	0.01	0.45	0.06	42.49	95.40	0.85	0.28	0.01	0.85	3
	14	0.00	0.01	0.02	0.01	0.00	46.28	0.02	0.47	0.08	45.73	92.62	0.00	0.01	0.02	0.01	0.00	41.08	5.78	0.02	0.47	0.08	45.73	93.20	0.93	0.12	0.01	0.93	3
Fig. 4 (6)	1	0.00	0.00	0.02	0.02		88.60	0.00		0.03	2.17	90.83	0.00	0.00	0.02	0.02	0.00	1.90	96.32	0.00	0.00	0.03	2.17	100.45	0.04	1.91	0.00	0.04	3
	2	0.00	0.00	0.04	0.01		88.18	0.00		0.03	2.38	90.64	0.00	0.00	0.04	0.01	0.00	2.09	95.64	0.00	0.00	0.03	2.38	100.19	0.05	1.90	0.00	0.05	3
	3	0.30	0.00	0.00	0.21		86.95	0.00		0.03	3.24	90.73	0.30	0.00	0.00	0.21	0.00	3.00	93.26	0.00	0.00	0.03	3.24	100.04	0.07	1.85	0.02	0.06	3
	4	0.00	0.00	0.00	0.02		86.88	0.00		0.04	2.72	89.66	0.00	0.00	0.00	0.02	0.00	2.43	93.82	0.00	0.00	0.04	2.72	99.03	0.05	1.89	0.00	0.05	3
	5	0.00	0.02	0.02	0.03		82.84	0.00		0.04	8.82	91.76	0.00	0.02	0.02	0.03	0.00	7.86	83.30	0.00	0.00	0.04	8.82	100.09	0.17	1.65	0.00	0.17	3
	6	0.53	0.00	0.04	0.02		82.80	0.00		0.03	7.55	90.96	0.53	0.00	0.04	0.02	0.00	7.35	83.83	0.00	0.00	0.03	7.55	99.33	0.16	1.67	0.02	0.15	3
Fig. 4 (7)	1	0.00	5.25	1.01	0.00		63.40	0.53		0.03	21.61	91.84	0.00	5.25	1.01	0.00	0.00	9.06	60.38	0.53	0.00	0.03	21.61	97.87	0.19	1.16	0.29	0.41	3
	2	0.00	3.82	0.73	0.01		56.26	0.50		0.06	30.38	91.75	0.00	3.82	0.73	0.01	0.00	19.77	40.54	0.50	0.00	0.06	30.38	95.80	0.43	0.79	0.21	0.59	3
	3	0.00	2.96	0.53	0.01		56.13	0.43		0.00	32.30	92.35	0.00	2.96	0.53	0.01	0.00	23.24	36.54	0.43	0.00	0.00	32.30	96.00	0.51	0.72	0.16	0.63	3
Fig. 4 (8)	1	0.00	1.19	0.62	0.00		58.49	0.52		0.00	30.43	91.26	0.00	1.19	0.62	0.00	0.00	24.61	37.64	0.52	0.00	0.00	30.43	95.02	0.55	0.76	0.09	0.61	3
	2	0.02	1.76	1.12	0.01		53.30	0.44		0.03	35.74	92.41	0.02	1.76	1.12	0.01	0.00	27.88	28.24	0.44	0.00	0.03	35.74	95.23	0.62	0.56	0.12	0.71	3

TABLE V. CALCULATED DIFFERENT MINERAL COMPONENT FRACTIONS OF THE SPOTS OF THE VARIOUS TITANHEMATITE EXSOLVED INTERGROWN GRAINS OF FIGURE 4

Grain	Spot	SiO_2	MgO	MnO	CaO	ZnO	FeO	Fe_2O_3	Al_2O_3	V_2O_3	Cr_2O_3	TiO_2	Total	Method	Gek	Pyr	Ilm	H	R	Total
Fig. 4 (1)	1	0.08	0.00	0.00	0.00	0.00	0.40	98.29	0.00	0.03	0.02	0.35	99.18	M2	0.00	0.00	0.66	98.41	0.00	99.07
	2	0.00	0.00	0.06	0.01	0.00	0.05	98.70	0.00	0.04	0.06	0.14	99.04	M1	0.00	0.12	0.11	98.76	0.01	99.00
	3	0.00	0.01	0.05	0.01	0.01	0.11	98.64	0.00	0.06	0.00	0.23	99.12	M1	0.04	0.10	0.23	98.64	0.03	99.03
	4	0.10	0.02	0.00	0.01	0.00	0.28	98.86	0.00	0.07	0.01	0.24	99.59	M2	0.07	0.00	0.36	99.04	0.00	99.47
	5	0.00	0.03	0.03	0.06	0.00	0.08	99.25	0.00	0.03	0.06	0.26	99.80	M1	0.10	0.05	0.16	99.31	0.08	99.70
	6	0.00	0.00	0.07	0.00	0.00	0.22	101.11	0.00	0.02	0.05	0.33	101.80	M1	0.01	0.14	0.47	101.16	0.00	101.78
Fig. 4 (2)	1	0.00	0.00	0.03	0.00	0.05	0.07	97.40	0.00	0.20	0.00	0.17	97.92	M1	0.00	0.07	0.15	97.40	0.05	97.67
	2	0.00	0.00	0.00	0.00	0.04	0.12	98.01	0.01	0.19	0.04	0.17	98.57	M1	0.00	0.00	0.26	98.05	0.03	98.35
	3	0.00	0.01	0.03	0.02	0.00	0.31	98.01	0.00	0.18	0.04	0.42	99.02	M1	0.02	0.06	0.66	98.05	0.02	98.82
	4	0.00	0.00	0.07	0.00	0.00	0.31	98.60	0.00	0.19	0.02	0.42	99.61	M1	0.00	0.15	0.65	98.62	0.00	99.42
	5	0.02	0.00	0.04	0.02	0.04	0.23	99.76	0.00	0.20	0.03	0.35	100.68	M1	0.00	0.08	0.49	99.79	0.04	100.41
Fig. 4 (3)	1	0.33	0.24	0.04	0.09	0.00	1.14	94.77	0.30	0.36	0.12	1.49	98.90	M2	0.73	0.09	1.82	95.57	0.00	98.22
	2	0.00	0.01	0.07	0.04	0.14	0.85	95.76	0.01	0.31	0.03	1.22	98.43	M1	0.02	0.14	1.79	95.80	0.19	97.95
	3	0.02	0.01	0.04	0.04	0.05	0.95	96.03	0.03	0.31	0.05	1.20	98.73	M1	0.02	0.08	2.02	96.12	0.08	98.32
	4	0.02	0.00	0.07	0.04	0.00	0.81	96.39	0.03	0.34	0.06	0.99	98.74	M1	0.00	0.14	1.70	96.47	0.02	98.34
Fig. 4 (4)	1	0.00	0.05	2.77	0.03	0.07	41.90	0.60	0.00	0.41	0.05	49.90	95.77	M1	0.15	5.88	88.50	0.65	0.11	95.29
	2	0.03	0.07	2.88	0.00	0.00	41.86	1.37	0.00	0.37	0.03	49.87	96.49	M2	0.21	6.12	88.34	1.46	0.00	96.13
	3	5.64	0.96	0.06	0.11	0.00	5.60	75.75	0.84	0.77	0.08	0.86	90.67	M2	2.86	0.12	0.00	82.95	0.00	85.93
	4	0.20	0.05	0.02	0.04	0.00	0.96	87.06	0.02	0.74	0.08	0.97	90.14	M2	0.14	0.04	1.62	87.36	0.00	89.16
	5	0.16	0.02	0.02	0.06	0.00	0.90	87.46	0.04	0.78	0.11	0.94	90.49	M2	0.05	0.05	1.67	87.77	0.00	89.54
	6	0.16	0.04	0.04	0.07	0.07	1.04	87.43	0.07	0.72	0.05	1.22	90.89	M2	0.10	0.07	2.11	87.60	0.00	89.89
	7	0.24	0.06	0.00	0.04	0.00	0.86	88.33	0.08	0.70	0.03	0.81	91.13	M2	0.16	0.00	1.33	88.72	0.00	90.21
	8	0.31	0.06	0.06	0.07	0.03	0.82	88.91	0.09	0.78	0.03	0.81	91.94	M2	0.17	0.13	1.19	89.34	0.00	90.83
	9	0.12	0.02	0.05	0.06	0.00	0.72	89.12	0.07	0.75	0.08	0.82	91.80	M2	0.06	0.11	1.38	89.42	0.00	90.97
	10	0.21	0.02	0.02	0.05	0.08	0.95	88.91	0.09	0.69	0.06	0.98	92.07	M2	0.05	0.04	1.75	89.24	0.00	91.08
	11	0.21	0.01	0.00	0.06	0.04	1.13	88.94	0.04	0.69	0.04	1.12	92.28	M2	0.02	0.00	2.09	89.21	0.00	91.33
	12	0.14	0.04	0.01	0.04	0.00	0.80	89.77	0.05	0.73	0.08	0.83	92.48	M2	0.11	0.02	1.43	90.04	0.00	91.59
	13	0.20	0.04	0.08	0.06	0.00	0.83	89.99	0.05	0.74	0.08	0.91	92.99	M2	0.11	0.17	1.41	90.29	0.00	91.98
Fig. 4 (5)	1	0.00	0.09	0.22	0.02	0.07	6.99	81.89	0.06	0.28	0.12	8.29	98.03	M1	0.26	0.47	14.76	82.07	0.10	97.66
	2	0.00	0.06	0.16	0.01	0.05	7.35	81.79	0.03	0.33	0.09	8.53	98.40	M1	0.19	0.34	15.53	81.90	0.06	98.02
	3	0.00	0.09	0.28	0.00	0.07	7.24	81.60	0.05	0.33	0.10	8.61	98.35	M1	0.28	0.58	15.28	81.74	0.07	97.96
	4	0.00	0.09	0.17	0.01	0.04	7.52	81.63	0.07	0.29	0.06	8.78	98.66	M1	0.26	0.37	15.89	81.75	0.05	98.32
	5	0.00	0.09	0.20	0.00	0.05	7.83	80.60	0.06	0.28	0.05	9.15	98.31	M1	0.26	0.43	16.54	80.71	0.05	97.99
	6	0.01	0.04	0.09	0.00	0.01	21.48	50.59	0.04	0.29	0.06	24.05	96.66	M1	0.12	0.19	45.37	50.69	0.00	96.36
	7	0.00	0.01	0.11	0.01	0.00	22.25	49.01	0.02	0.37	0.09	24.90	96.77	M1	0.04	0.23	47.00	49.12	0.02	96.40
	8	0.00	0.04	0.08	0.00	0.00	25.13	41.34	0.03	0.43	0.05	28.10	95.20	M1	0.10	0.18	53.07	41.42	0.00	94.78
	9	0.00	0.01	0.07	0.00	0.00	26.27	38.44	0.02	0.44	0.09	29.28	94.61	M1	0.01	0.14	55.47	38.55	0.00	94.18
	10	0.00	0.01	0.05	0.01	0.01	27.77	34.80	0.04	0.39	0.11	30.96	94.14	M1	0.02	0.10	58.66	34.94	0.02	93.74
	11	0.00	0.00	0.08	0.01	0.01	31.53	26.25	0.04	0.39	0.08	35.16	93.55	M1	0.00	0.17	66.59	26.37	0.03	93.15
	12	0.00	0.00	0.07	0.00	0.03	33.31	22.55	0.04	0.48	0.07	37.13	93.67	M1	0.00	0.14	70.34	22.66	0.03	93.18
	13	0.00	0.02	0.04	0.01	0.00	38.13	14.19	0.01	0.45	0.06	42.49	95.40	M1	0.05	0.09	80.54	14.26	0.01	94.96
	14	0.00	0.01	0.02	0.01	0.00	41.08	5.78	0.02	0.47	0.08	45.73	93.20	M1	0.04	0.04	86.76	5.88	0.02	92.73
Fig. 4 (6)	1	0.00	0.00	0.02	0.02		1.90	96.32	0.00		0.03	2.17	100.45	M1	0.00	0.04	4.02	96.34	0.03	100.43
	2	0.00	0.00	0.04	0.01		2.09	95.64	0.00		0.03	2.38	100.19	M1	0.00	0.09	4.41	95.67	0.01	100.18
	3	0.30	0.00	0.00	0.21		3.00	93.26	0.00		0.03	3.24	100.04	M2	0.00	0.00	6.15	93.41	0.00	99.56
	4	0.00	0.00	0.00	0.02		2.43	93.82	0.00		0.04	2.72	99.03	M1	0.00	0.00	5.13	93.86	0.02	99.02
	5	0.00	0.02	0.02	0.03		7.86	83.30	0.00		0.04	8.82	100.09	M1	0.04	0.04	16.60	83.35	0.03	100.06
	6	0.53	0.00	0.04	0.02		7.35	83.83	0.00		0.03	7.55	99.33	M2	0.00	0.09	14.25	84.54	0.00	98.88
Fig. 4 (7)	1	0.00	5.25	1.01	0.00		9.06	60.38	0.53		0.03	21.61	97.87	M1	15.66	2.15	19.13	60.94	0.04	97.91
	2	0.00	3.82	0.73	0.01		19.77	40.54	0.50		0.06	30.38	95.80	M1	11.39	1.54	41.75	41.10	0.04	95.82
	3	0.00	2.96	0.53	0.01		23.24	36.54	0.43		0.00	32.30	96.00	M1	8.81	1.12	49.08	36.98	0.04	96.03
	4	0.00	1.26	0.28	0.02		31.35	0.00	0.19		0.00	62.23	95.33	M3	3.76	0.58	0.00	35.03	59.43	98.80
	5	0.00	0.96	0.20	0.03		23.93	0.00	0.17		0.02	70.07	95.37	M3	2.86	0.43	0.00	26.78	67.95	98.01
	6	0.01	1.35	0.31	0.01		24.06	0.00	0.17		0.00	70.37	96.27	M3	4.01	0.65	0.00	26.91	67.37	98.95
	7	0.00	0.90	0.23	0.01		16.52	0.00	0.09		0.05	78.69	96.49	M3	2.68	0.49	0.00	18.50	76.65	98.33
	8	0.00	0.71	0.20	0.01		13.70	0.00	0.08		0.00	82.42	97.12	M3	2.11	0.43	0.00	15.30	80.80	98.64
Fig. 4 (8)	1	0.00	1.19	0.62	0.00		24.61	37.64	0.52		0.00	30.43	95.02	M1	3.56	1.32	51.98	38.16	0.02	95.03
	2	0.02	1.76	1.12	0.01		27.88	28.24	0.44		0.03	35.74	95.23	M1	5.25	2.38	58.89	28.71	0.00	95.23

TABLE VI. MICROPROBE CHEMICAL ANALYSIS AND MOLECULAR FORMULAE OF THE SPOTS OF THE FERROMAGNETIC TITANHEMATITE EXSOLVED INTERGROWN GRAINS OF FIGURE 5

Grains	Spot	SiO_2	MgO	MnO	CaO	ZnO	FeO	Al_2O_3	V_2O_3	Cr_2O_3	TiO_2	Total	SiO_2	MgO	MnO	CaO	ZnO	FeO	Fe_2O_3	Al_2O_3	V_2O_3	Cr_2O_3	TiO_2	Total	Ferrous Fe	Ferric Fe	Other cations	Ti	O
Fig. 5 (1)	1	6.66	0.49	0.03	0.15	0.01	78.05	2.09	0.29	0.04	0.20	88.00	6.66	0.49	0.03	0.15	0.01	7.03	78.90	2.09	0.29	0.04	0.20	95.88	0.16	1.57	0.37	0.00	3
	2	0.51	0.00	0.00	0.07	0.17	86.16	0.08	0.27	0.04	0.57	87.86	0.51	0.00	0.00	0.07	0.17	0.88	94.74	0.08	0.27	0.04	0.57	97.32	0.02	1.94	0.04	0.01	3
	3	0.38	0.05	0.00	0.03	0.00	88.97	0.04	0.29	0.03	0.11	89.90	0.38	0.05	0.00	0.03	0.00	0.43	98.36	0.04	0.29	0.03	0.11	99.73	0.01	1.97	0.03	0.00	3
	4	0.29	0.03	0.03	0.00	0.01	89.02	0.00	0.26	0.02	0.18	89.84	0.29	0.03	0.03	0.00	0.01	0.40	98.45	0.00	0.26	0.02	0.18	99.68	0.01	1.97	0.02	0.00	3
	5	0.80	0.00	0.02	0.00	0.00	89.19	0.00	0.30	0.07	0.33	90.71	0.80	0.00	0.02	0.00	0.00	1.23	97.72	0.00	0.30	0.07	0.33	100.4	0.03	1.94	0.04	0.01	3
	6	0.12	0.01	0.05	0.02	0.00	89.67	0.00	0.29	0.07	0.24	90.48	0.12	0.01	0.05	0.02	0.00	0.26	99.34	0.00	0.29	0.07	0.24	100.4	0.01	1.98	0.02	0.00	3
	7	0.00	0.01	0.00	0.00	0.00	94.07	0.00	0.28	0.03	0.23	94.62	0.00	0.01	0.00	0.00	0.00	0.20	104.2	0.00	0.28	0.03	0.23	105.0	0.00	1.98	0.01	0.00	3
Fig. 5 (2)	1	0.06	0.00	0.11	0.00	0.00	87.62	0.01	0.06	0.09	0.89	88.83	0.06	0.00	0.11	0.00	0.00	0.76	96.50	0.01	0.06	0.09	0.89	98.47	0.02	1.96	0.01	0.02	3
	2	0.06	0.01	0.23	0.00	0.00	88.24	0.00	0.05	0.03	0.22	88.84	0.06	0.01	0.23	0.00	0.00	0.02	98.01	0.00	0.05	0.03	0.22	98.63	0.00	1.99	0.01	0.00	3
	3	0.00	0.00	0.19	0.00	0.12	92.38	0.00	0.12	0.01	0.35	93.16	0.00	0.00	0.19	0.00	0.12	0.01	102.6	0.00	0.12	0.01	0.35	103.4	0.00	1.98	0.01	0.01	3
	4	0.00	0.02	0.19	0.00	0.09	92.78	0.00	0.06	0.00	0.27	93.41	0.00	0.02	0.19	0.00	0.09	-0.07	103.1	0.00	0.06	0.00	0.27	103.7	0.00	1.99	0.01	0.01	3
Fig. 5 (3)	1	0.02	2.63	0.81	0.00	0.05	76.05	2.50	0.70	0.07	13.6	96.51	0.02	2.63	0.81	0.00	0.05	6.78	76.96	2.50	0.70	0.07	13.6	104.2	0.14	1.41	0.26	0.25	3
	2	0.08	2.42	0.93	0.01	0.00	74.54	0.93	0.75	0.00	14.8	94.48	0.08	2.42	0.93	0.01	0.00	8.18	73.72	0.93	0.75	0.00	14.8	101.8	0.17	1.39	0.20	0.28	3
	3	0.04	2.19	0.79	0.02	0.13	71.90	1.64	0.75	0.03	16.2	93.76	0.04	2.19	0.79	0.02	0.13	9.85	68.94	1.64	0.75	0.03	16.2	100.6	0.21	1.31	0.22	0.31	3
	4	0.08	2.13	0.86	0.00	0.14	73.17	1.50	0.71	0.00	16.3	94.93	0.08	2.13	0.86	0.00	0.14	9.98	70.20	1.50	0.71	0.00	16.3	101.9	0.21	1.32	0.21	0.31	3
	5	0.05	2.32	0.98	0.00	0.18	72.44	1.23	0.71	0.04	17.0	94.97	0.05	2.32	0.98	0.00	0.18	10.0	69.26	1.23	0.71	0.04	17.0	101.8	0.21	1.30	0.21	0.32	3
	6	0.12	0.83	0.20	0.03	0.15	66.73	1.30	0.87	0.08	22.9	93.23	0.12	0.83	0.20	0.03	0.15	18.9	53.11	1.30	0.87	0.08	22.9	98.54	0.41	1.04	0.12	0.45	3
	7	0.06	1.28	0.15	0.01	0.09	65.40	1.98	0.85	0.02	23.8	93.69	0.06	1.28	0.15	0.01	0.09	19.0	51.53	1.98	0.85	0.02	23.8	98.84	0.41	1.00	0.16	0.46	3
	8	0.08	0.89	0.20	0.01	0.09	65.09	1.53	0.91	0.02	24.1	93.01	0.08	0.89	0.20	0.01	0.09	19.9	50.15	1.53	0.91	0.02	24.1	98.02	0.43	0.98	0.13	0.47	3
	9	0.07	1.29	0.45	0.01	0.05	64.66	1.16	0.84	0.01	25.7	94.30	0.07	1.29	0.45	0.01	0.05	20.4	49.12	1.16	0.84	0.01	25.7	99.21	0.44	0.95	0.14	0.50	3
	10	0.10	0.92	0.30	0.03	0.09	65.40	1.10	0.87	0.06	26.1	95.04	0.10	0.92	0.30	0.03	0.09	21.6	48.64	1.10	0.87	0.06	26.1	99.90	0.46	0.94	0.12	0.50	3
	11	0.06	1.65	0.36	0.00	0.16	61.06	2.94	0.93	0.04	26.5	93.69	0.06	1.65	0.36	0.00	0.16	20.4	45.09	2.94	0.93	0.04	26.5	98.19	0.44	0.87	0.21	0.51	3
	14	0.06	0.34	0.16	0.01	0.00	47.19	0.49	1.01	0.04	44.3	93.65	0.06	0.34	0.16	0.01	0.00	39.1	8.90	0.49	1.01	0.04	44.3	94.54	0.87	0.18	0.06	0.89	3
Fig. 5 (4)	3	0.14	0.05	0.02	0.04	0.00	85.83	0.01	0.32	0.09	4.28	90.77	0.14	0.05	0.02	0.04	0.00	3.87	91.06	0.01	0.32	0.09	4.28	99.86	0.09	1.81	0.02	0.09	3
	4	0.03	0.04	0.07	0.00	0.00	86.01	0.00	0.35	0.10	3.97	90.57	0.03	0.04	0.07	0.00	0.00	3.47	91.70	0.00	0.35	0.10	3.97	99.73	0.08	1.83	0.02	0.08	3
Fig. 5 (5)	6	0.02	0.00	0.00	0.01		84.72	0.00		0.01	8.77	93.53	0.02	0.00	0.00	0.01	0.00	7.90	85.35	0.00	0.00	0.01	8.77	102.0	0.17	1.66	0.00	0.17	3
	7	0.00	0.02	0.00	0.00		83.29	0.00		0.00	9.55	92.86	0.00	0.02	0.00	0.00	0.00	8.56	83.02	0.00	0.00	0.00	9.55	101.1	0.19	1.63	0.00	0.19	3
	8	0.01	0.00	0.00	0.04		82.65	0.02		0.02	9.41	92.14	0.01	0.00	0.00	0.04	0.00	8.43	82.47	0.02	0.00	0.02	9.41	100.3	0.18	1.63	0.00	0.19	3
	9	0.03	0.01	0.02	0.03		77.55	0.00		0.01	17.8	95.43	0.03	0.01	0.02	0.03	0.00	15.9	68.39	0.00	0.00	0.01	17.8	102.2	0.34	1.31	0.00	0.34	3
	10	0.28	0.05	0.00	0.03		73.08	0.06		0.02	19.5	93.07	0.28	0.05	0.00	0.03	0.00	17.7	61.44	0.06	0.00	0.02	19.5	99.21	0.39	1.21	0.02	0.39	3
Fig. 5 (6)	1	0.04	2.99	1.39	0.02	0.28	73.61	1.82	0.47	0.03	13.4	94.07	0.04	2.99	1.39	0.02	0.28	5.12	76.10	1.82	0.47	0.03	13.4	101.6	0.11	1.43	0.28	0.25	3
	2	0.02	2.25	1.03	0.08	0.13	72.32	1.14	0.43	0.05	16.5	94.03	0.02	2.25	1.03	0.08	0.13	9.68	69.60	1.14	0.43	0.05	16.5	100.9	0.20	1.32	0.20	0.32	3
	3	0.08	2.43	0.99	0.04	0.21	71.22	1.49	0.46	0.05	18.0	95.06	0.08	2.43	0.99	0.04	0.21	10.7	67.14	1.49	0.46	0.05	18.0	101.7	0.23	1.26	0.22	0.34	3
	4	0.01	2.10	1.06	0.04	0.14	69.14	1.09	0.51	0.02	18.5	92.63	0.01	2.10	1.06	0.04	0.14	11.7	63.82	1.09	0.51	0.02	18.5	99.00	0.25	1.24	0.19	0.36	3
	5	0.03	1.74	0.73	0.01	0.14	69.80	0.81	0.50	0.03	19.7	93.56	0.03	1.74	0.73	0.01	0.14	13.8	62.16	0.81	0.50	0.03	19.7	99.77	0.30	1.20	0.15	0.38	3
	6	0.06	1.56	0.61	0.03	0.00	70.56	0.44	0.53	0.00	20.4	94.24	0.06	1.56	0.61	0.03	0.00	15.0	61.69	0.44	0.53	0.00	20.4	100.4	0.32	1.19	0.12	0.39	3
	7	0.00	2.03	1.18	0.02	0.21	67.25	1.27	0.52	0.05	22.0	94.62	0.00	2.03	1.18	0.02	0.21	14.8	58.22	1.27	0.52	0.05	22.0	100.4	0.31	1.11	0.19	0.42	3
	8	0.23	2.42	0.76	0.01	0.12	63.46	0.99	0.48	0.08	22.9	91.53	0.23	2.42	0.76	0.01	0.12	15.7	52.99	0.99	0.48	0.08	22.9	96.82	0.34	1.04	0.20	0.45	3
	9	0.01	1.88	0.94	0.00	0.18	63.04	1.04	0.52	0.00	24.3	91.97	0.01	1.88	0.94	0.00	0.18	17.4	50.62	1.04	0.52	0.00	24.3	97.02	0.38	1.00	0.17	0.48	3
	10	0.03	0.89	0.34	0.03	0.00	44.02	0.41	0.64	0.00	47.7	94.11	0.03	0.89	0.34	0.03	0.00	41.0	3.32	0.41	0.64	0.00	47.7	94.44	0.91	0.07	0.07	0.95	3
	11	0.35	0.08	0.19	0.19	0.16	39.37	0.39	0.59	0.16	49.2	90.67	0.35	0.08	0.19	0.19	0.16	39.4	0.00	0.39	0.59	0.16	49.2	90.70	0.88	0.00	0.05	1.03	3
	12	0.05	0.76	0.23	0.03	0.00	44.18	0.34	0.60	0.00	49.3	95.59	0.05	0.76	0.23	0.03	0.00	42.8	1.50	0.34	0.60	0.00	49.3	95.74	0.94	0.03	0.06	0.97	3

VI. CONCLUSION

The high purity Egyptian beach ilmenite concentrate contains several mineral textures. The rutile-ilmenite exsolved intergrowths are far less common than in titanhematite. In this exsolved intergrowth, the ilmenite component is a ferriilmenite composed of 31.68-80.47% ilmenite, 0.4-33.2% hematite, 1.79-35.78% geikielite, 0.64-2.34% pyrophanite, and 0.02-0.29% rutile. The Cr_2O_3 contents range between 0 and 0.5%. The other component of the intergrowth is ferriferrous rutile, consisting of 57.5-87.41% rutile, 8.23-33.86% hematite, 0.42-16.55% geikielite, and 0.20-1.70% pyrophanite, while the Cr_2O_3 content ranges between 0 and 0.4%. In these intergrowths, the content of the included hematite in the ferriilmenite component, decreases, as the geikielite ($MgTiO_3$) and/or pyrophanite ($MnTiO_3$) contents increase. MgO and MnO mix easier with ilmenite rather than with hematite.

On the other hand, the relatively larger and darker exsolved rutile bodies are composed mainly of rutile (more than 95% TiO_2), while the relatively smaller ones are mainly ferriferrous rutile with considerable amounts of mixed hematite.

It was noticed that the ilmenite enriched with relatively higher content of MgO and individual TiO_2 is unstable and alters partially into rutile and hematite. Increased TiO_2 content leads to the exsolution of rutile bodies. The difference in the geometry of the associated mixed mineral crystal structures and their corresponding contents inside the rutile-ilmenite exsolved intergrowth in addition to the prevailing physical conditions may be responsible of the different obtained textures of such intergrowth.

The titanhematite intergrowth includes 3 fabrics arranged in a decreasing order of abundance as: ilmenite-hematite, rutile-hematite, and rutile-ilmenite-hematite. The TiO_2 content attains up to 9.15%. Both MgO and MnO have minimum values and do not follow Fe_2O_3. In the titanhematite host, MgO ranges between 0 and 0.2%, while MnO ranges between 0 and 0.3%. Only in the case of exsolved rutile within the titanhematite host, the titanhematite host contained MgO ranges between 1.2 and 5.3%, while the MnO content ranges between 0.5 and 1.1%. The exsolved rutile MgO content ranges between 0.6 and 1.3%, while the MnO content ranges between 0.2 and 0.7%.

It was found that the contained exsolved ilmenite may be altered into pseudorutile or mixed rutile and hematite fabric. In some homogeneous titanhematite or mixed rutile-hematite, the Fe_2O_3 content can be replaced with SiO_2. In all types of the titanhematite intergrowth, the Cr_2O_3 contents range between 0 and 0.1%.

TABLE VII. CALCULATED DIFFERENT MINERAL COMPONENT FRACTIONS OF THE SPOTS OF THE VARIOUS FERROMAGNETIC TITANHEMATITE EXSOLVED INTERGROWN GRAINS OF FIGURE 5

Grain	Spot	SiO_2	MgO	MnO	CaO	ZnO	FeO	Fe_2O_3	Al_2O_3	V_2O_3	Cr_2O_3	TiO_2	Total	Method	Gek	Pyr	Ilm	H	R	Total
Fig. 5 (1)	1	6.66	0.49	0.03	0.15	0.01	7.03	78.90	2.09	0.29	0.04	0.20	95.88	M2	1.47	0.07	0.00	90.24		91.77
	2	0.51	0.00	0.00	0.07	0.17	0.88	94.74	0.08	0.27	0.04	0.57	97.32	M2	0.01	0.00	1.07	95.33		96.40
	3	0.38	0.05	0.00	0.03	0.00	0.43	98.36	0.04	0.29	0.03	0.11	99.73	M2	0.15	0.00	0.03	98.94		99.12
	4	0.29	0.03	0.03	0.00	0.01	0.40	98.45	0.00	0.26	0.02	0.18	99.68	M2	0.10	0.07	0.15	98.91		99.22
	5	0.80	0.00	0.02	0.00	0.00	1.23	97.72	0.00	0.30	0.07	0.33	100.47	M2	0.00	0.05	0.58	98.88		99.51
	6	0.12	0.01	0.05	0.02	0.00	0.26	99.34	0.00	0.29	0.07	0.24	100.40	M2	0.03	0.11	0.31	99.58		100.03
	7	0.00	0.01	0.00	0.00	0.00	0.20	104.29	0.00	0.28	0.03	0.23	105.04	M1	0.01	0.00	0.42	104.32	0.00	104.76
Fig. 5 (2)	1	0.06	0.00	0.11	0.00	0.00	0.76	96.50	0.01	0.06	0.09	0.89	98.47	M2	0.00	0.24	1.46	96.74		98.44
	2	0.06	0.01	0.23	0.00	0.00	0.02	98.01	0.00	0.05	0.03	0.22	98.63	M2	0.01	0.49	0.00	97.99		98.50
	3	0.00	0.00	0.19	0.00	0.12	0.01	102.61	0.00	0.12	0.01	0.35	103.41	M1	0.00	0.41	0.03	102.62	0.11	103.17
	4	0.00	0.02	0.19	0.00	0.09	-0.07	103.16	0.00	0.06	0.00	0.27	103.72	M2	0.06	0.41	0.01	103.14		103.63
Fig. 5 (3)	1	0.02	2.63	0.81	0.00	0.05	6.78	76.96	2.50	0.70	0.07	13.67	104.20	M1	7.85	1.72	14.31	79.54	0.04	103.45
	2	0.08	2.42	0.93	0.01	0.00	8.18	73.72	0.93	0.75	0.00	14.83	101.84	M2	7.21	1.98	17.11	74.70		101.00
	3	0.04	2.19	0.79	0.02	0.13	9.85	68.94	1.64	0.75	0.03	16.27	100.65	M1	6.52	1.68	20.79	70.61	0.12	99.72
	4	0.08	2.13	0.86	0.00	0.14	9.98	70.20	1.50	0.71	0.00	16.34	101.94	M1	6.36	1.83	21.09	71.70	0.06	101.03
	5	0.05	2.32	0.98	0.00	0.18	10.09	69.26	1.23	0.71	0.04	17.03	101.89	M1	6.92	2.07	21.32	70.53	0.13	100.97
	6	0.12	0.83	0.20	0.03	0.15	18.93	53.11	1.30	0.87	0.08	22.93	98.54	M1	2.48	0.43	39.98	54.49	0.02	97.39
	7	0.06	1.28	0.15	0.01	0.09	19.02	51.53	1.98	0.85	0.02	23.85	98.84	M1	3.81	0.31	40.16	53.54	0.03	97.85
	8	0.08	0.89	0.20	0.01	0.09	19.95	50.15	1.53	0.91	0.02	24.18	98.02	M1	2.67	0.43	42.14	51.70	0.01	96.95
	9	0.07	1.29	0.45	0.01	0.05	20.45	49.12	1.16	0.84	0.01	25.76	99.21	M1	3.84	0.95	43.19	50.29	-0.01	98.26
	10	0.10	0.92	0.30	0.03	0.09	21.62	48.64	1.10	0.87	0.06	26.18	99.90	M1	2.74	0.63	45.66	49.80	0.00	98.83
	11	0.06	1.65	0.36	0.00	0.16	20.47	45.09	2.94	0.93	0.04	26.50	98.19	M1	4.92	0.75	43.23	48.07	0.09	97.07
	14	0.06	0.34	0.16	0.01	0.00	39.18	8.90	0.49	1.01	0.04	44.35	94.54	M2	1.02	0.34	82.63	9.49		93.48
Fig. 5 (4)	3	0.14	0.05	0.02	0.04	0.00	3.87	91.06	0.01	0.32	0.09	4.28	99.86	M2	0.13	0.05	7.91	91.29		99.38
	4	0.03	0.04	0.07	0.00	0.00	3.47	91.70	0.00	0.35	0.10	3.97	99.73	M2	0.11	0.14	7.26	91.92		99.42
Fig. 5 (5)	1	0.01	0.00	0.00	0.02		0.46	0.00	0.00		0.02	100.16	100.67		0.00	0.00		0.53	100.16	100.69
	2	0.00	0.00	0.02	0.03		0.44	0.00	0.00		0.02	99.91	100.44		0.01	0.05		0.51	99.88	100.45
	3	0.00	0.00	0.00	0.00		0.55	0.00	0.00		0.05	99.88	100.47		0.00	0.01		0.65	99.87	100.53
	4	0.14	0.00	0.00	0.09		0.51	0.00	0.00		0.03	99.57	100.33		0.00	0.00		0.59	99.57	100.16
	5	0.14	0.01	0.00	0.07		0.51	0.00	0.00		0.04	99.66	100.42		0.02	0.00		0.60	99.64	100.27
	6	0.02	0.00	0.00	0.01	0.00	7.90	85.35	0.00	0.00	0.01	8.77	102.06	M2	0.00	0.00	16.66	85.40		102.06
	7	0.00	0.02	0.00	0.00	0.00	8.56	83.02	0.00	0.00	0.00	9.55	101.15	M1	0.05	0.00	18.08	83.02	0.00	101.15
	8	0.01	0.00	0.00	0.04	0.00	8.43	82.47	0.02	0.00	0.02	9.41	100.38	M1	0.00	0.00	17.79	82.50	0.05	100.34
	9	0.03	0.01	0.02	0.03	0.00	15.99	68.39	0.00	0.00	0.01	17.80	102.27	M1	0.01	0.03	33.77	68.40	0.00	102.21
	10	0.28	0.05	0.00	0.03	0.00	17.78	61.44	0.06	0.00	0.02	19.54	99.21	M2	0.16	0.00	36.93	61.86		98.95
Fig. 5 (6)	1	0.04	2.99	1.39	0.02	0.28	5.12	76.10	1.82	0.47	0.03	13.43	101.67	M1	8.92	2.96	10.81	77.94	0.28	100.90
	2	0.02	2.25	1.03	0.08	0.13	9.68	69.60	1.14	0.43	0.05	16.59	100.98	M1	6.71	2.20	20.43	70.78	0.23	100.35
	3	0.08	2.43	0.99	0.04	0.21	10.79	67.14	1.49	0.46	0.05	18.08	101.77	M1	7.25	2.11	22.80	68.68	0.17	101.00
	4	0.01	2.10	1.06	0.04	0.14	11.70	63.82	1.09	0.51	0.02	18.53	99.00	M1	6.26	2.24	24.71	64.93	0.19	98.33
	5	0.03	1.74	0.73	0.01	0.14	13.85	62.16	0.81	0.50	0.03	19.78	99.77	M1	5.20	1.56	29.25	63.00	0.12	99.12
	6	0.06	1.56	0.61	0.03	0.00	15.04	61.69	0.44	0.53	0.00	20.46	100.40	M2	4.65	1.29	31.72	62.13		99.80
	7	0.00	2.03	1.18	0.02	0.21	14.84	58.22	1.27	0.52	0.05	22.09	100.44	M1	6.07	2.52	31.34	59.54	0.25	99.71
	8	0.23	2.42	0.76	0.01	0.12	15.77	52.99	0.99	0.48	0.08	22.99	96.82	M2	7.21	1.61	32.98	54.26		96.06
	9	0.01	1.88	0.94	0.00	0.18	17.48	50.62	1.04	0.52	0.00	24.37	97.02	M1	5.60	1.99	36.92	51.66	0.17	96.34
	10	0.03	0.89	0.34	0.03	0.00	41.03	3.32	0.41	0.64	0.00	47.76	94.44	M1	2.65	0.72	86.65	3.73	0.01	93.77
	11	0.35	0.08	0.19	0.19	0.16	39.40	0.00	0.39	0.59	0.16	49.21	90.16	M2	0.23	0.39	83.21	0.54	5.05	89.43
	12	0.05	0.76	0.23	0.03	0.00	42.84	1.50	0.34	0.60	0.00	49.38	95.74	M1	2.28	0.49	90.47	1.84	0.00	95.07

TABLE VIII. ORIGINAL MICROPROBE CHEMICAL ANALYSIS OF SOME SPOTS OF THE GRAINS FROM FIGURES 4, 5

Grain	Spot	SiO_2	MgO	MnO	CaO	ZnO	FeO	Fe_2O_3	Al_2O_3	V_2O_3	Cr_2O_3	TiO_2	Total
Fig. 4 (3)	5	96.02	0.16	0.00	0.04	0.00	1.72	0.00	0.81	0.03	0.00	0.36	99.14
	6	0.32	0.03	0.22	54.49	0.67	2.33	0.00	0.00	0.04	0.05	0.11	58.25
	7	0.21	0.00	0.10	55.49	0.72	1.96	0.00	0.00	0.04	0.00	0.07	58.59
Fig. 4 (6)	7	37.45	0.01	0.18	23.10		14.45	0.00	22.45		0.04	0.10	97.78
	8	49.84	0.04	0.19	19.54		10.26	0.00	19.14		0.03	0.09	99.13
	9	90.85	0.00	0.00	0.16		1.13	0.00	0.03		0.01	8.51	100.68
	10	85.10	0.13	0.00	0.07		0.78	0.00	0.90		0.02	17.19	104.19
	11	63.75	0.91	0.00	0.19		2.25	0.00	1.71		0.00	28.06	96.87
	12	5.57	0.02	0.00	0.11		1.29	0.00	0.68		0.03	94.98	102.69
	13	93.90	0.17	0.00	1.28		1.21	0.00	3.08		0.03	0.09	99.75
Fig. 4 (8)	3	0.00	0.57	0.29	0.02		29.92	0.00	0.22		0.04	63.66	94.72
	4	0.00	1.05	0.69	0.01		28.45	0.00	0.23		0.00	64.72	95.15
	5	0.01	0.63	0.50	0.00		23.35	0.00	0.18		0.00	69.55	94.22
	6	50.05	3.08	0.12	0.30		11.12	0.00	21.99		0.00	1.67	88.33
Fig. 5 (3)	12	0.00	1.9	0.5	0.00	0.1	53.4	0.0	3.5	0.8	0.0	33.4	93.8
	13	0.0	1.4	0.3	0	0.1	53.5	0.0	2.5	0.9	0.0	35.8	94.6
Fig. 5 (4)	1	0.89	0.03	0.00	0.10	0.00	57.48	0.00	0.64	0.47	0.11	31.91	91.62
	2	0.93	0.00	0.04	0.02	0.00	63.20	0.00	0.00	0.39	0.07	26.75	91.39
	5	0.34	0.10	0.09	54.08	0.62	1.98	0.00	0.00	0.01	0.01	0.30	57.53
Fig. 5 (5)	11	11.57	1.24	0.04	0.20		2.83	0.00	8.35		0.00	58.65	82.88
Fig. 5 (6)	13	0.03	0.60	0.25	0.01	0.03	37.93	0.00	0.25	0.59	0.00	56.80	96.50
	14	1.27	0.23	0.04	44.53	0.29	4.51	0.00	0.06	0.10	0.02	5.94	57.00

Some ferromagnetic titanhematite varieties separated from the fraction of magnetite are detected. They are produced by the martitization of titanomagnetite. Their TiO_2 content attains up to 24.37%. In these grains, the contents of Cr_2O_3, MgO, and MnO range between 0.0-0.2, 0.0-3, and 0.0-1.4% respectively. In fact, some of the exsolved intergrown textures included within the grains of the ilmenite concentrate contain relatively higher values of Cr_2O_3 content, their distribution is relatively lower, and they are the only reason for the increased Cr_2O_3 content in the obtained ilmenite concentrate. In fact, several varieties of chromite and chromspinel mineral grains are found and represent 1.1% of the detected bulk ilmenite grains. In these grains, the contents of Cr_2O_3, MgO, V_2O_3, and Al_2O_3 range between 16.69-56.72, 0.54-17.33, 0.14-0.58, and 1.33-38.79% respectively.

Although it is rarely met with one of these high chromium grains within the ilmenite concentrate, the relatively finer grain sizes of most of them could led to the separation for some of them to ilmenite rather than to separated ferromagnetic fractions. Especially with the current used types of magnetic separators. Hence, the problem of high Cr_2O_3 content of the Egyptian beach ilmenite concentrate is an ore dressing problem rather than a mineralogical one.

One of the most important conclusions is that in the case of the ilmenite of the El Burullus-Baltim sand dunes, it is expected that a considerable fraction of ilmenite can be obtained with relatively lower Cr_2O_3 content. The reason for this is that most of the heavy and economic interesting minerals are concentrated in relatively coarser grain sizes than those of beach sediments. So, the associated relatively finer chromite and chromspinel grains will be in minimum contents.

ACKNOWLEDGEMENT

The author wishes to express his appreciation to the Deputyship for Research & Innovation, Ministry of Education, Saudi Arabia for funding this research work.

REFERENCES

[1] A. A. Mahessar *et al.*, "Sediment Transport Dynamics in the Upper Nara Canal Off-taking from Sukkur Barrage of Indus River," *Engineering, Technology & Applied Science Research*, vol. 10, no. 6, pp. 6563–6569, Dec. 2020, https://doi.org/10.48084/etasr.3924.

[2] E. M. Kara, M. Meghachou, and N. Aboubekr, "Contribution of Particles Size Ranges to Sand Friction," *Engineering, Technology & Applied Science Research*, vol. 3, no. 4, pp. 497–501, Aug. 2013, https://doi.org/10.48084/etasr.361.

[3] N. P.H. Padmanabhan, T. Sreenivas, and N. K. Rao, "Processing of Ores of Titanium, Zirconium, Hafnium, Niobium, Tantalum, Molybdenum, Rhenium, and Tungsten: International Trends and the Indian Scene," *High Temperature Materials and Processes*, vol. 9, no. 2–4, pp. 217–248, Jul. 1990, https://doi.org/10.1515/HTMP.1990.9.2-4.217.

[4] A. Stwertka, *A guide to the elements*. Oxford, England: Oxford University Press, 1998.

[5] F. Habashi, *Principles of Extractive Metallurgy: Pyrometallurgy*. Oxford, UK: Gordon and Breach, 1993.

[6] E. Barbara and S. Hawkins, Eds., "Thorium and Thorium Compounds to Vitamins," in *Ullmann's Encyclopedia of Industrial Chemistry*, vol. A27, 1996, pp. 95–122.

[7] T. S. Mackey, "Upgrading ilmenite into a high-grade synthetic rutile," *JOM*, vol. 46, no. 4, pp. 59–64, Apr. 1994, https://doi.org/10.1007/BF03220676.

[8] A.-A. M. Abdel-Karim, S. M. Zaid, M. I. Moustafa, and M. G. Barakat, "Mineralogy, chemistry and radioactivity of the heavy minerals in the black sands, along the northern coast of Egypt," *Journal of African Earth Sciences*, vol. 123, pp. 10–20, Nov. 2016, https://doi.org/10.1016/j.jafrearsci.2016.07.005.

[9] A.-A. M. Abdel-Karim, M. I. Moustafa, A. H. El-Afandy, and M. G. Barakat, "Mineralogy, Chemical Characteristics and Upgrading of Beach Ilmenite of the Top Meter of Black Sand Deposits of the Kafr Al-Sheikh Governorate, Northern Egypt," *Acta Geologica Sinica*, vol. 91, no. 4, pp. 1326–1338, 2017, https://doi.org/10.1111/1755-6724.13364.

[10] A. A. Dewedar, "Comparative studies on the heavy minerals in some black sands deposits from Sinai and east Rosetta with contribution to the mineralogy and economics of their garnets," Ph.D. dissertation, El Menoufia University, Shibin El Kom, Egypt, 1997.

[11] A. A. El-Kammar, A. A. Ragab, and M. I. Moustafa, "Geochemistry of economic heavy minerals from Rosetta black sand of Egypt," *Journal of King Abdulaziz University: Earth Sciences*, vol. 22, no. 2, pp. 69–97, 2011, https://doi.org/10.4197/Ear.22-2.4.

[12] N. M. Hammoud, "Concentration of monazite from Egyptian black sands, employing industrial techniques," M.S. thesis, Cairo University, Giza, Egypt, 1966.

[13] N. M. S. Hammoud, "A process for recovery of low chromium high grade ilmenite from north Egyptian beach deposits," in *Proceedings, 11th Indust. Mineral Process Conference*, Sardegna, Italy, 1975.

[14] M. A. Mikhail, "Distribution and sedimentation of ilmenite in black sands, west of Rosetta," M.S. thesis, Cairo University, Cairo, Egypt, 1971.

[15] M. I. Moustafa, "Mineralogy and beneficiation of some economic minerals in the Egyptian black sands," Ph.D. dissertation, Mansoura University, Mansoura, Egypt, 1999.

[16] R. M. Tyler and R. C. A. Minnitt, "A review of sub-Saharan heavy mineral sand deposits : implications for new projects in southern Africa," *Journal of the Southern African Institute of Mining and Metallurgy*, vol. 104, no. 2, pp. 89–99, Mar. 2004, https://doi.org/10.10520/AJA0038223X_2869.

[17] M. A. Mandour, T. Chernet, and M. I. Moustafa, "Applied mineralogical studies on Egyptian sand ilmenite concentrates," in *Seventh Biennial Sgs Meeting on Mineral Exploration and Sustainable Development*, Athens, Greece, 2003, pp. 903–906.

[18] M. F. R. Fouda, R. S. Amin, H. I. Saleh, A. A. Labib, and H. A. Mousa, "Preparation and characterization of nanosized Titania prepared from beach black sands broad on Mediterranean Sea Coast in Egypt Via reaction with acids," *Australian Journal of Basic Applied Sciences*, vol. 4, no. 10, pp. 4540–4553, 2010.

[19] N. A. El-Hussiny, T. A. Lasheen, and M. E. H. Shalabi, "Kinetic reduction of Rosetta ilmenite with coke Breeze and Beneficiation of the product," *The Journal of ORE DRESSING*, vol. 10, no. 20, pp. 16–23, Jan. 2008.

[20] M. I. Moustafa, M. A. Tashkandi, and A. M. El-Sherif, "Detecting Mineral Resources and Suggesting a Physical Concentration Flowsheet for Economic Minerals at the Northern Border Region of Saudi Arabia," *Engineering, Technology & Applied Science Research*, vol. 12, no. 3, pp. 8617–8627, Jun. 2022, https://doi.org/10.48084/etasr.4894.

[21] M. I. Moustafa, "Some Mineralogical Characteristics of the Egyptian Black Sand Beach Ilmenite: Homogeneous Ilmenite and Titanhematite-Ferriilmenite Grains-Part I," *Engineering, Technology & Applied Science Research*, vol. 12, no. 6, pp. 9614-9631, Dec. 2022, https://doi.org/10.48084/etasr.5296.

[22] E. F. Stumpfl, "Erzmikroskopische untersuchungen an schwermineralien in sanden," *Geol.Jarb*, vol. 73, pp. 685–723, 1958.

[23] E. Z. Basta and M. A. Takla, "Mineralogy and Origin of Abu Ghalaga Ilmenite Occurrence, Eastern Desert," *Journal of Geology*, vol. 12, no. 2, pp. 87–124, 1968.

[24] N. K. Rao and G. V. U. Rao, "Intergrowths in ilmenite of the beach sands of Kerala," *Mineralogical magazine and journal of the Mineralogical Society*, vol. 35, no. 269, pp. 118–130, Mar. 1965, https://doi.org/10.1180/minmag.1965.035.269.14.

[25] E. Z. Basta, "New Data on the System Fe2O3- FeTiO3-TiO2 (Ferri-Ilmenite and Titanom-agetite)," *Proceeding Egyptian Academic Science*, vol. 14, pp. 1–15, 1959.

[26] P. Ramdohr, *Die Erzmineralien in gewohnlichen magmatischen Gesteinen*. Berlin, Germany: Verlag der Wissenschaften, 1940.

[27] J. R. Balsley and A. F. Buddington, "Iron-titanium oxide minerals, rocks, and aeromagnetic anomalies of the Adirondack area, New York," *Economic Geology*, vol. 53, no. 7, pp. 777–805, Nov. 1958, https://doi.org/10.2113/gsecongeo.53.7.777.

[28] W. Uytenbogaardt, *Tables for microscopic identification of ore minerals,* Second Edition. Amsterdam, Netherlands: Elsevier, 1971.

[29] S. E. Haggerty, "Oxide textures; a mini-atlas," *Reviews in Mineralogy and Geochemistry*, vol. 25, no. 1, pp. 129–219, Jan. 1991.

[30] P. Ramdohr, *The Ore Minerals and Their Intergrowths*. Oxford, UK: Pergamon Press, 1980.

[31] A. B. Edwards, *Textures of the ore minerals and their significance.* Melbourne, VIC, Australia: Australasian Institute of Mining and Metallurgy, 1947.

[32] P. Ramdohr, *Die Beziehungen von Fe-Ti-Erzen aus magmatischen Gesteinen*. Valtioneuvoston kirjapaino, 1956.